

UNIVERSITY OF STAVANGER

**Dopamine as a Homeostatic Regulator
of Levodopa and its contribution to
Neurological Disorders**

by

Olga Afradi

Bachelor Thesis in Biological Chemistry

submitted to the

Faculty of Science and Technology

Department of Biology, Chemistry and Environmental Engineering

May 2021

"Theory is when you know everything but nothing works. Practice is when everything works but no one knows why. In the laboratory, theory and practice are combined: Nothing works and no one knows why."

Unknown author

UNIVERSITY OF STAVANGER

Abstract

Faculty of Science and Technology

Department of Biology, Chemistry and Environmental Engineering

Bachelor Thesis in Biological Chemistry

by Olga Afradi

Homeostasis is the tendency to maintain a relatively constant internal environment. The concept of homeostasis is essential when it comes to understanding organisms and their ability to adapt when faced with external changes. Integral control can be implemented by three conditions. These are zero-order, first-order and second-order kinetics. Time-dependent perturbations are rapidly increased to study whether the controlled variable can be kept at a set-point. The ideal behavior of a controller would be that step-wise perturbations drive the controller back to its theoretical set-point. The results presents how integral control and negative feedback are key features when determining the performance of a controller. In this thesis we study the performance of negative feedback controllers. Dopamine (DA) plays a significant role in homeostatically regulating Levodopa (L-DOPA/DOPA) through these negative feedback mechanisms. The importance of this regulation is highlighted in the thesis because small dysregulations of DOPA has seemingly proven to be the source of several neurological disorders. The controllers are able to deal with different time-dependent perturbations. However, when facing concentration values in either a too high or too low degree, the controller has a disadvantage of breaking down. The implementation of compensatory values were included to test whether the reaction could return to set-point.

Acknowledgements

I would like to express my special thanks of gratitude to my supervisor professor Dr. Peter Ruoff as well as professor Dr. Qaiser Waheed. You have both given me the golden opportunity to do this wonderful project on the topic "Homeostasis". Thank you for providing useful research topics.

It has been a great privilege and honour to work and study under your guidance. I am deeply honoured to be a part of such a meaningful research project.

Finally, I would also like to thank my family and friends who supported me in finalizing this project within the limited time frame. Additional thanks to my mother who reviewed this thesis.

Contents

Abstract	ii
Acknowledgements	iii
List of Figures	vi
1 Introduction	1
1.1 About homeostasis	1
1.2 The story behind the concept	1
1.3 Feedback mechanisms and integral control	2
1.4 Dopamine homeostasis	4
1.5 Goal of this work	5
2 Materials and Methods	6
3 Results and Discussion	8
3.1 Experimental scheme of Model 1	8
3.1.1 Experimentally determined values and graphical outputs	9
3.1.2 Regulation of Tyr, DOPA and DA by altering k_1	11
3.1.3 Negative feedback mechanisms leads to accumulated levels of Dopamine	12
3.1.4 Broken homeostasis by the alteration of V_{max} of VAT2	16
3.1.5 Set-point changes results in preserved homeostasis	20
3.2 Tyrosine Hydroxylase and its two catalyzation functions	23
3.2.1 Parkinson's Disease is highly connected to TH regulation	24
3.2.2 Tyrosine Hydroxylase and its effect on maximum velocity	24
3.2.3 DA regulates TH through competitive inhibition	25
3.2.4 TH alters V_{max} of VAT2 into achieving homeostatic control	27
3.2.5 DOPA is not homeostatically regulated by the presence of TH when k_{11} is altered	29
3.3 An overview scheme	31
3.3.1 Negative feedback mechanisms focuses mainly on DOPA regulation	32
3.3.2 VAT2 has a heavy impact upon DA in the vesicle pool	35
3.3.3 A broader view of the inflow of DA	36
3.4 DOPA as a treatment method	37
3.4.1 DA restores DOPA homeostasis	37

3.4.2	DOPA regulates oxidative stress	38
3.5	MATLAB calculations	39
3.6	Conclusion	40

Bibliography	42
---------------------	-----------

List of Figures

1.1	Scheme that illustrates integral control. A , the controlled variable, is regulated to set-point (A_{set}). This happens even though A is exposed to uncontrolled perturbations. The calculation and integration of e regulates A into reaching A_{set} -value. E is integrated in \dot{E}	3
1.2	Overview scheme of how Dopamine is regulated in the cell. First, Phenylalanine is converted into Tyrosine. Second, Tyrosine is converted to DOPA by Tyrosine Hydroxylase (TH). Finally, aromatic amino acid decarboxylase (DDC) converts DOPA to Dopamine.	4
3.1	Reaction scheme for Model 1.	8
3.2	The experimental determined concentration values of constants k_1 - k_{14} presented in input file for Model 1 (left). The label "TH7-01" refers to the models run-id. The concentrations of each constant are the same for all three phases. These are changed later on. Summary of the compilation is presented in the column to the right.	10
3.3	Graphic results when Model 1 was compiled. All constant values are the same for all three phases, as this model is used as a reference model. Phase 1, 2 and 3 are color coded with arrows. (a) k_9 values remains constant at around $5.00 \mu M$. (b) DA (blue) is unchanged at $292.00 \mu M$, and DOPA (red) around value $5.39 \mu M$ (c) Tyrosine is also unchanged around $157.50 \mu M$	11
3.4	Results when k_1 was altered in Model 1. (a) Tyrosine levels (yellow) showed a steady, linear increase as higher k_1 values was applied. (b) Dopamine (blue) experienced a rapid increase, peaking at value $300 \mu M$, before decreasing at a high rate until k_1 equaled $20 \mu M/min$. (c) Steady-state value of DOPA (black) was reached until $k_1=20 \mu M/min$. DOPA set values (red) is here used as a constant.	11
3.5	Competitive inhibition scheme [1]. The enzyme and substrate either forms the traditional enzyme-substrate complex (ES) or enzyme-inhibitor complex (EI). Latter reaction is reversible.	12
3.6	Results when k_4 (inhibition constant) was altered in Model 1. (a) Dopamine experienced a steady, linear increase, reaching values as far as $1300 \mu M$ when $k_4=200 \mu M/min$. (b) Steady-state values of DOPA remained unchanged throughout the reaction, implying preserved homeostasis.	13
3.7	Results when k_{12} (inhibition constant) was altered in Model 1. (a) Dopamine experienced a steady, slightly curved increase as higher constant values was applied. (b) Steady-state values of DOPA (black) fluctuated in an increasing manner, suggesting struggles of upholding a homeostatic environment. Meanwhile, DOPA set-point (red) remained constant at concentration $5.38 \mu M$	14

3.8	Substrate inhibition scheme [2]. The enzyme has in this case catalytic activity when one substrate is bound, but no activity if two are bound.	14
3.9	Results when the k_7 -constant was decreased by 50% ($k_7=0.75 \mu M$) in Model 1. DOPA levels were heavily decreased in phase 2. Meanwhile, Dopamine concentration were increased to an extreme extent, peaking at $7000 \mu M$. The graphs of all compounds had slow incline/decline in phase 3 as time went by. This slow uptake before reaching steady-state revealed that homeostasis was broken.	16
3.10	Exponential increase in DOPA set-point (Equation 3.14) as a function of k_7 . Values $k_5=3.1 \mu M$, $k_6=28.0 \mu M$ and $k_{11}=1.0 \mu M$ are inserted.	18
3.11	Results when $k_7=0.75 \mu M$ in phase 2 and $k_7=2.25 \mu M$ in phase 3. This ended in a quicker response time in contrast to when $k_7=0.75 \mu M$ only in phase 2.	19
3.12	Results when the k_{11} -constant was increased by 50% ($k_{11}=1.5 \mu M$). DOPA levels became highly decreased in phase 2. Meanwhile, Dopamine concentrations experienced a towering high level around the same time interval. Tyrosine levels increased in the same phase, followed by a slow decline in phase 3. The time-slowness in phase 3 revealed that homeostasis was not maintained.	20
3.13	Decrease in DOPA set-point (Equation 3.16) as a function of k_{11} . Values $k_5=3.1 \mu M$, $k_6=28.0 \mu M$ and $k_7=1.5 \mu M$ are inserted.	21
3.14	Results when Hypothesis 1 was applied in the goal of testing whether two contrast constant values would make the cell adjust itself into a more homeostatic environment. k_{11} was set to $1.5 \mu M$ in phase 2 and $0.5 \mu M$ in phase 3. DOPA, Dopamine and Tyrosine revealed a shorter time response in phase 3.	22
3.15	Scheme of Model 2. TH catalyzes the turnover of both Tyrosine and DOPA.	23
3.16	Results when V_{max}/k_2 had initial value of $k_2=20 \mu M$. The constant was changed to $k_2=40 \mu M$ in phase 2. DOPA levels had a slight increase in phase 2 before it became stabilized in phase 3. Both Dopamine and Tyrosine seemed to experience difficulties in achieving homeostasis in the third phase.	25
3.17	Comparison of Model 1 and Model 2 when k_4 was altered. The figure illustrates how TH-expression in the scheme of Model 2 overall affected the outcome of Tyr, DA and DOPA. (a) Model 1 showed a linear increase in DA and reached values up to $1400 \mu M$ at a relatively high rate. Meanwhile Model 2 had steady and low concentration values throughout the simulation ($0.00073 \mu M$). (b) DOPA steady-state and set-point value was maintained at a constant level for both Model 1 and Model 2.	26
3.18	Comparison of Model 2 and Model 1 when k_7 (V_{max} of VAT2) was altered. (a) DA decreased in both simulations. However, Model 2 required application of way higher k_7 -concentrations to experience even a slight decrease in DA outcome. (b) DOPA had earlier expressed unregulated homeostasis as a result of changed steady-state values in Model 1. Model 2 showed results that now was homeostatically regulated now that a new behaviour of TH was introduced. DOPA concentration remained stabilized and unchanged.	28

3.19	Results on Model 2 when k_{11} was increased by 50% like in Figure 3.12 (Model 1). The concentration value was set to $k_{11}=1.5 \mu M$ in phase 2. Dopamine and Tyrosine were both heavily increased in the second phase and decreased in phase 3. DOPA levels sunk in phase 2 followed by a shift in phase 3.	30
3.20	Model 3 presents a broader view of the Dopamine reaction pathway. An overview of how the nerve impulse is carried and released into the synaptic cleft is shown. The reaction is also extended to depict how Dopamine receives negative feedback from auto-receptors. At last it is shown how Dopamine re-enters the cells internal environment.	32
3.21	Results on Model 3 when k_4 was increased to $90 \mu M$ in phase 2. A drastic increase of DOPA occurred in phase 2 as DA levels slightly shifted to higher values in the same time interval. Both DOPA and DA in the cytosol encountered slightly difficulties in becoming stabilized, unlike external DA (DA_{ext}) and DA in the vesicle ($DA_{vesicle}$) who both eventually reached steady-state in phase 3. Tyrosine concentration decreased in phase 2, but its levels quickly accumulated in the last phase.	33
3.22	This figure illustrated what happened when k_{20} was changed to $0.2 \mu M$ in phase 2. Interestingly, DOPA concentrations were decreased throughout all three phases at the same time as the amount of DA in cytosol expressed almost unchanged values. DOPA values were almost completely aligned with set-values ($DOPA_{set}$) in the third phase, implying that homeostasis was maintained. Meanwhile, Tyrosine levels had an increase in phase 3.	34
3.23	The alteration of V_{max} of VAT2. $k_7=0.75 \mu M$ was applied in the second phase. The DA-levels in the vesicle ($DA_{vesicle}$) and in the synaptic cleft (DA_{ext}) was instantly decreased throughout this phase and encountered struggles in returning to set-point in the third phase.	35
3.24	Results when k_{11} was changed from $1.0 \mu M$ to $2.0 \mu M$ in Model 3. The increase of inflow resulted in wavering levels of $DOPA_{set}$ throughout phase 1 and 2, followed by a slow regulation into steady-state in phase 3. DOPA concentration was decreased during phase 2 and encountered struggles in stabilizing in phase 3. External DA shifted to lowered values in phase 2, but stabilized in phase 3. Tyrosine levels accumulated throughout the same time period, especially in phase 2.	36
3.25	Reaction scheme for Model 4. Rate constant k_{22} represents an additional inflow of DOPA from an external source (green).	37
3.26	Results on Model 4 when k_{22} was changed to $2 \mu M$ in phase 2, expressing a continuous flow of DOPA into the reaction. Dopamine levels were increased in phase 2 as a result, which enabled DOPA to become homeostatically regulated. This event occurred in phase 3, and is confirmed by the steady values of $DOPA_{set}$	38
3.27	Results on Model 4 when $k_{22}=12 \mu M$ and $k_{14}=0.15 \mu M$ in phase 2. Dopamine levels were increased, which in turn restored DOPA homeostasis.	39
3.28	Comparison of MATLAB and Fortran results on k_4 with time interval $t=[100,300]$ (phase 2 in Fortran). Tyrosine decreased during this time period. DOPA was first heavily increased, and experienced a slow decline in concentration levels after 120 min. DA increased linearly.	40

3.29 Comparison of MATLAB and Fortran results on k_7 with time interval $t=[200,400]$ (phase 2 in Fortran). Tyrosine increased throughout the reaction. DOPA experienced a decrease. Lastly, DA levels were increased linearly.	40
---	----

For the future of science...

Chapter 1

Introduction

1.1 About homeostasis

Homeostasis is the term for regulation of the physical and chemical state in organisms. The article “Fysiologiske reguleringsmekanismer” states this concept as “keeping something approximately constant” [3]. The main purpose is to keep individuals adapted to external environment changes. An example of this is regulation of different physiological aspects in the human body. These aspects include temperature, blood sugar, blood pressure, respiration, fluid balance and pH balance. The components stated cooperate in maintaining a constant internal environment.

There are three key regulator components of homeostasis [4]. First of all, we have sensors that detects different stimuli. The stimuli then affect a control center, which generates a certain output. At last, a response is triggered. The response is mostly a physiological activity that helps the environment return to a desired value. An example of this is when the temperature decreases in a heating system at home. A temperature monitored by a sensor drop would act as a stimulus and activate the thermostat. In this situation the control center will increase the heat until the desired temperature is reached. The response is produced by the heater.

1.2 The story behind the concept

The regulation mechanisms of internal environment were first described by the French physiologist Claude Bernard in 1849 [5]. His studies were based on experiments which led him to discover the pancreas’ influence on the metabolism. Glycogen, a source of energy in animals, seemed to play an important role in the overall regulation. The

discovery of this carbohydrate along with its way of assembling and self-destruction in the cells, also known as glycogen metabolism, proved that the body itself produced chemical compounds. Later, Bernard also discovered how certain nerves regulated the blood flow in the organs. He reported that the heat increased as he cut sympathetic fibers joining the sympathetic ganglia, followed by a more active circulation of the blood in the arteries [5]. This phenomenon was an example of how the body quickly adapted to maintain a constant internal environment.

Walter Bradford Cannon improved and narrowed down Bernard's studies about regulation of the internal environment, also known as "le milieu interieur". He introduced the term "homeostasis" in 1926. Cannon presented four propositions to describe the general features of homeostasis [6]. These included the fact that (1) mechanisms adjust to maintain stability, (2) factors resist change when it happens, (3) mechanisms can act together and that (4) mechanisms are mostly organized, and do not occur by chance.

In later studies of homeostasis, it has become more usual to describe the regulation mechanisms through certain mathematical models used in computational biology [3]. These models are the foundation of how scientist today carry out research in the hopes of discovering how homeostasis plays an important role in development of disease and the understanding of physiological regulation.

1.3 Feedback mechanisms and integral control

Communication among cells is necessary to maintain internal stability. Feedback mechanisms are key controllers of the homeostatic processes in the body. Their main goal is to influence the function of one final component by reading conditions of an initial component. These mechanisms participate in the communicative systems of the body like the nervous and endocrine system. Components such as chemical messengers and hormones travel through the extracellular fluid while carrying information that trigger responses in target cells [7]. The results of the feedback mechanisms have either an increasing or decreasing effect on the system.

We distinguish between negative and positive feedback mechanisms. Negative feedback systems uphold stability and equilibrium by inhibiting certain changes. Inhibition controls prevents excessive responses to the stimulus. The difference between positive and negative feedback is that a positive feedback system enhances the response when stimulated [7].

In living organisms, robustness is provided by homeostatic mechanisms in order to survive and reproduce. Robustness of a system is defined as "the ability of tolerating

perturbations that might affect the system's functional body" [8]. When facing external variations, robustness is achieved by maintaining homeostasis. Integral feedback is a control-engineering concept that plays an important role in adapting and achieving a robust environment [9]. The perks of an integral control system is that it can keep a system at a given set-point, even when exposed to uncontrollable perturbations.

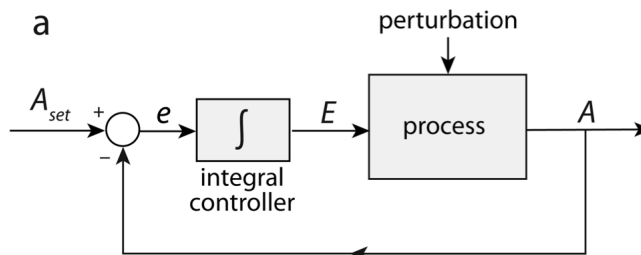


FIGURE 1.1: Scheme that illustrates integral control. A , the controlled variable, is regulated to set-point (A_{set}). This happens even though A is exposed to uncontrolled perturbations. The calculation and integration of e regulates A into reaching A_{set} -value. E is integrated in \dot{E} .

The rate equations of Figure 1.1 are:

$$\dot{A} = k_1 - k_2 \cdot A - k_4 \cdot A + \frac{k_3 \cdot K_i}{K_i + E} \quad (1.1)$$

$$\dot{E} = k_5 \cdot A - \frac{V_{max} \cdot E}{K_M + E} \quad (1.2)$$

where $k_2 \cdot A$ describes the perturbation and $K_i + E$ represents the compensatory flux.

The steady state value in A (A_{ss}) is described by the set-point (setting $\dot{E}=0$ and $\dot{A}=0$, thereby solving for A_{ss}):

$$A_{ss} = A_{set} = \frac{V_{max}}{k_5} \quad (1.3)$$

By solving with respect to $\dot{E}(=0)$ we get the expression:

$$\dot{E} = -k_5 \left(\frac{V_{max}}{k_5} - A \right) \quad (1.4)$$

By replacing V_{max}/k_5 with A_{set} we get an equation which signifies that \dot{E} is proportional to the error and that E is integrated in \dot{E} :

$$e = A_{set} - A \quad (1.5)$$

A_{set} represents the set-point and A is the controlled variable. The negative feedback loop regulates the integral controller. e defines the error between A and A_{set} .

1.4 Dopamine homeostasis

Regulation of Dopamine homeostasis is controlled by mentioned feedback systems. Dopamine plays several important roles in the brain and body [10]. It functions as a neurotransmitter, a chemical released by neurons. The chemicals travel through several distinct Dopamine pathways throughout the body. Reward-motivated behavior is a result of increased level of Dopamine in the brain.

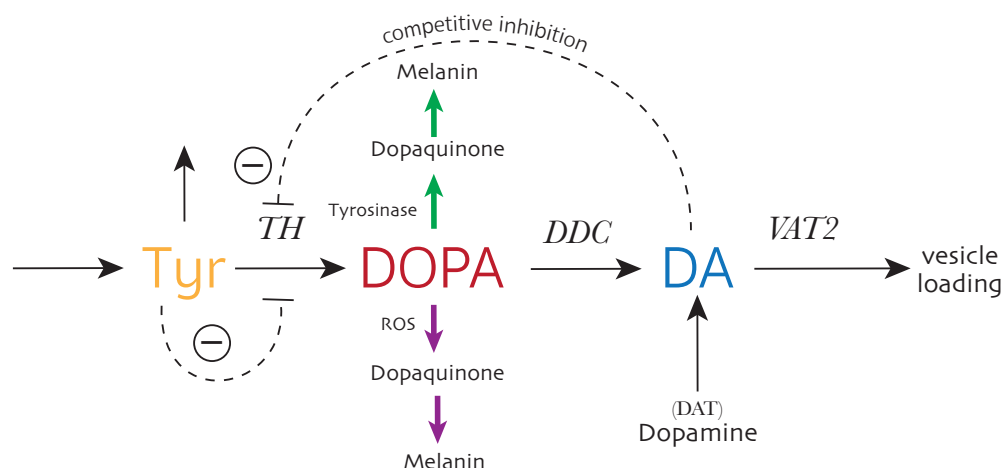


FIGURE 1.2: Overview scheme of how Dopamine is regulated in the cell. First, Phenylalanine is converted into Tyrosine. Second, Tyrosine is converted to DOPA by Tyrosine Hydroxylase (TH). Finally, aromatic amino acid decarboxylase (DDC) converts DOPA to Dopamine.

Homeostasis of Dopamine is achieved through a series of compounds working together. The precursors Tyrosine and DOPA work together with the enzymes Tyrosine Hydroxylase (TH), DOPA Decarboxylase (DDC) and vesicular monoamine transporter 2 (VAT2) in a reaction pathway to maintain Dopamine homeostasis.

Small dysregulations in the dopamine homeostatic pathway can result in severe damage to the human body. An example of a disorder linked to this phenomenon are Dopamine dysregulation syndrome, which often occurs in people who have Parkinson's disease. This disease affects the motor system, resulting in cognitive and behavioral problems

presented in the symptoms of tremor, rigidity, slowness of movement and difficulty with walking [11].

1.5 Goal of this work

The goal of this thesis was to discover how far the concentrations in the cell could be altered in order to maintain or break homeostasis. Experiments on Dopamine were executed on programming models assisted by computational methods. Concentration constants were altered in the purpose of gaining insight on how Tyrosine (Tyr), Levodopa (DOPA) and Dopamine (DA) were affected in the different cases. The computational experiments were compared to earlier scientific studies in the purpose of discovering how and why Dopamine functions as a homeostatic regulator of DOPA. The results were further integrated in the discussion section, which elaborated on how a dysregulated system could contribute to neurological disorders. At last, simulations were performed to theoretically determine whether DOPA could serve as a treatment option for these disorders.

Chapter 2

Materials and Methods

Scientific programming tools were the main source of presented calculations and simulations. Data was extracted using Perl (v. 5.28.2) as the main programming language. Graphs were constructed in gnuplot (www.gnuplot.info) and edited using Adobe Illustrator program v2021 (www.adobe.com). Scientific computing was carried out by Absoft's Pro Fortran compiler with subroutine LSODE [12]. The Fortran programs are named "TH7", "TH8", "TH9" and "TH10", but are here referred to as "Model 1", "Model 2", "Model 3" and "Model 4" in the "Results and Discussion" section. MATLAB (mathworks.com) was an additional tool which was used as a confirmation method of some of the Fortran calculations.

The rate constants used in the experiments (Results and Discussion) are presented in Figure 2.1:

TABLE 2.1: Rate constants used in the calculations.

Rate constants	Experimental value	Function	Reference
k_1	$5 \mu M$	V_{max} (flux)	[13]
k_2	$20 \mu M$	V_{max} (TH)	[14]
k_3	$74.4 \mu M$	K_m (TH)	[15]
k_4	$45 \mu M$	Inhibition constant (V_{max})	[16]
k_5	$3.1 \mu M$	V_{max} (DDC)	[17]
k_6	$28 \mu M$	K_m (DDC)	[18]
k_7	$1.5 \mu M$	V_{max} (VAT2)	[19]
k_8	$0.00029 \mu M$	K_m (VAT2)	[19]
k_9	$2.86 \mu M$	V_{max} (Tyrosinase)	[20]
k_{10}	$0.025 \mu M$	V_{max} (flux)	[13]
k_{11}	$1 \mu M$	V_{max} (flux, DA)	[19]
k_{12}	$50 \mu M$	Inhibition constant (V_{max})	[21]
k_{13}	$22 \mu M$	K_m (Tyrosinase)	[22]
k_{14}	$0 \mu M$	V_{max} (ROS)	[23]
k_{15}	$2.3 \mu M$	V_{max} (TH)	[20]
k_{16}	$50 \mu M$	K_m (TH)	[24]
k_{17}	$0.01 \mu M$	V_{max} (flux)	[19]
k_{18}	$100\ 000 \mu M$	V_{max} (MAO)	[25]
k_{19}	$100 \mu M$	K_m (MAO)	[25]
k_{20}	$0.1 \mu M$	Inhibition constant (V_{max})	[19]
k_{21}	$0.0001 \mu M$	K_m (flux)	[19]
k_{22}	$0 \mu M$	V_{max} (flux)	[26]

Chapter 3

Results and Discussion

3.1 Experimental scheme of Model 1

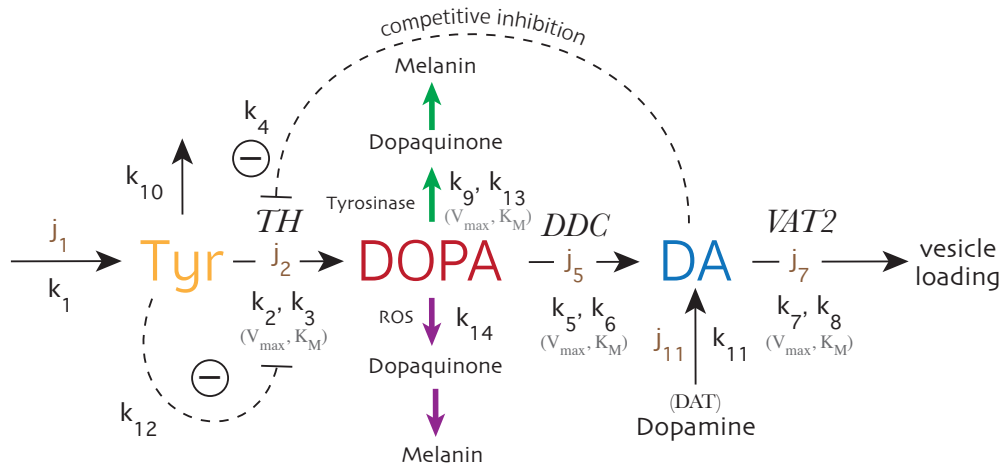


FIGURE 3.1: Reaction scheme for Model 1.

Figure 3.1 shows two different reaction pathways leading to melanin production. The first path is through Tyrosinase with the inclusion of V_{max} and K_M values for this enzyme. The other is guided via reactive oxygen species (ROS). Both pathways synthesize the precursor Dopaquinone, which forms melanin when oxidized. The depicted "j" 's are fluxes.

The simulations on Dopamine homeostasis showed interesting results. In almost all cases, homeostasis was preserved even though the constants were changed drastically. Exceptions occurred when constants k_7 and k_{11} were altered in Model 1. Homeostasis was clearly broken in these simulations. k_4 revealed some interesting results, which enlightened how negative feedback had an overall large impact on the Dopamine reaction

pathway. The results of the constant changes are further discussed in the following subsections. Main focus will be upon the three mentioned constants; the inhibition constant (k_4), the V_{max} -value of enzyme VAT2 (k_7) and lastly the j_{11} -flux (k_{11}).

The rate equations of the Tyrosine, DOPA and Dopamine are:

$$\frac{d(Tyr)}{dt} = \frac{k_2 \cdot Tyr}{k_3 \left(1 + \frac{DA}{k_4}\right) + Tyr} \cdot \frac{k_{12}}{k_{12} + Tyr} - k_{10} Tyr \quad (3.1)$$

$$\frac{d(DOPA)}{dt} = \frac{k_2 \cdot Tyr}{k_3 \left(1 + \frac{DA}{k_4}\right) + Tyr} \cdot \frac{k_{12}}{k_{12} + Tyr} - \frac{k_9 \cdot DOPA}{k_{13} + DOPA} - \frac{k_5 \cdot DOPA}{k_6 + DOPA} - k_{14} DOPA \quad (3.2)$$

$$\frac{d(DA)}{dt} = \frac{k_5 \cdot DOPA}{k_6 + DOPA} - \frac{k_7 \cdot DA}{k_8 + DA} \quad (3.3)$$

The expression of set-point is:

$$DOPA_{set} = \frac{k_6 \cdot (k_7 - k_{11})}{k_5 + k_4 - k_7} \quad (3.4)$$

3.1.1 Experimentally determined values and graphical outputs

Figure 3.2 and Figure 3.3 represent the experimentally determined values of Model 1, and is used as a reference model. These illustrate how a cell normally behaves when the constant values are the same for all three phases. Their original values are used for further comparison in the subsections to show how the cell changes when the constants are altered in phases 2 and 3. Phase 1 remains unchanged throughout all examples in the purpose of implementing a contrast between start-concentration and end-concentration. All concentrations are in μM . The graphs (Figure 3.3(a), 3.3(b) and 3.3(c)) was illustrated by Gnuplot when the experimental values were compiled in Terminal.

```

TH7-01
0.0000E+00, 1.0000E+0, 10000.0E+0, 20000.0E+0, 20000.0D+0

5.0E+00 ** k1 phase 1
2.0D+01 ** k2 phase 1
7.44E+1 ** k3 phase 1
45.0E+00 ** k4 phase 1
3.1D+00 ** k5 phase 1
2.8D+1 ** k6 phase 1
1.5D+00 ** k7 phase 1
0.29D-3 ** k8 phase 1
2.86 ** k9 phase 1
2.5D-02 ** K10 phase 1
1.0D+00 ** K11 phase 1
5.0D+01 ** K12 phase 1
2.2D+01 ** K13 phase 1
0.0D+00 ** K14 phase 1

5.0E+00 ** k1 phase 2
2.0D+01 ** k2 phase 2
7.44E+1 ** k3 phase 2
45.0E+00 ** k4 phase 2
3.1D+00 ** k5 phase 2
2.8D+1 ** k6 phase 2
1.5D+00 ** k7 phase 2
0.29D-3 ** k8 phase 2
2.86 ** k9 phase 2
2.5D-02 ** K10 phase 2
1.0D+00 ** K11 phase 2
5.0D+01 ** K12 phase 2
2.2D+01 ** K13 phase 2
0.0D+00 ** K14 phase 2

5.0E+00 ** k1 phase 3
2.0D+01 ** k2 phase 3
7.44E+1 ** k3 phase 3
45.0E+00 ** k4 phase 3
3.1D+00 ** k5 phase 3
2.8D+1 ** k6 phase 3
1.5D+00 ** k7 phase 3
0.29D-3 ** k8 phase 3
2.86 ** k9 phase 3
2.5D-02 ** K10 phase 3
1.0D+00 ** K11 phase 3
5.0D+01 ** K12 phase 3
2.2D+01 ** K13 phase 3
0.0D+00 ** K14 phase 3

0.0D+00 ** K9DOT used only in phase 2 for linear growth

1.575E+02, 5.385E+00, 2.919E+02 ** Tyr, DOPA, DA

0 ** NOUT

```

```

Phase 1
At end of phase 1 :
k1=j1..... 5.0000E+00
j2..... 1.0624E+00
j2 when DA=0..... 3.2731E+00
j2-j5-j9-j14..... 5.5708E-12
j5..... 5.0000E-01
j7..... 1.5000E+00
j9..... 5.6236E-01
j11=k11..... 1.0000E+00
j5+j11-j7..... -3.6606E-10
j14 (ROS)..... 0.0000E+00
k2 (Vmax,TH)..... 2.0000E+01
k3 (KM,TH)..... 7.4400E+01
k4 KI (DA)..... 4.5000E+01
k5 (Vmax, DDC)..... 3.1000E+00
k6 (KM, DDC)..... 2.8000E+01
k7 (Vmax,transport).... 1.5000E+00
k8 (KM, transport).... 2.9000E-04
k9 (Vmax tyrosinase)... 2.8600E+00
k10 Istore remove Tyr.. 2.5000E-02
k11 dopamine re-entry.. 1.0000E+00
k12 KI(Tyr) TH..... 5.0000E+01
k13 KM(DOPA) tyrosinase 2.2000E+01
k14 ROS DOPA pathway... 0.0000E+00
k6(k7-k11)/(k5+k11-k7). 5.3846E+00
Concentrations at end of phase 1 :
1.575E+02, 5.385E+00, 2.919E+02

Phase 2
At end of phase 2 :
k1=j1..... 5.0000E+00
j2..... 1.0624E+00
j2 when DA=0..... 3.2731E+00
j2-j5-j9-j14..... 7.2498E-14
j5..... 5.0000E-01
j7..... 1.5000E+00
j9..... 5.6236E-01
j11=k11..... 1.0000E+00
j5+j11-j7..... -4.7564E-12
j14 (ROS)..... 0.0000E+00
k2 (Vmax,TH)..... 2.0000E+01
k3 (KM,TH)..... 7.4400E+01
k4 KI (DA)..... 4.5000E+01
k5 (Vmax, DDC)..... 3.1000E+00
k6 (KM, DDC)..... 2.8000E+01
k7 (Vmax,transport).... 1.5000E+00
k8 (KM, transport).... 2.9000E-04
k9 (Vmax tyrosinase)... 2.8600E+00
k10 Istore remove Tyr.. 2.5000E-02
k11 dopamine re-entry.. 1.0000E+00
k12 KI(Tyr) TH..... 5.0000E+01
k13 KM(DOPA) tyrosinase 2.2000E+01
k14 ROS DOPA pathway... 0.0000E+00
k6(k7-k11)/(k5+k11-k7). 5.3846E+00
Concentrations at end of phase 2 :
1.575E+02, 5.385E+00, 2.919E+02

Phase 3
At end of phase 3 :
k1=j1..... 5.0000E+00
j2..... 1.0624E+00
j2 when DA=0..... 3.2731E+00
j2-j5-j9-j14..... 1.1102E-15
j5..... 5.0000E-01
j7..... 1.5000E+00
j9..... 5.6236E-01
j11=k11..... 1.0000E+00
j5+j11-j7..... -6.1950E-14
j14 (ROS)..... 0.0000E+00
k2 (Vmax,TH)..... 2.0000E+01
k3 (KM,TH)..... 7.4400E+01
k4 KI (DA)..... 4.5000E+01
k5 (Vmax, DDC)..... 3.1000E+00
k6 (KM, DDC)..... 2.8000E+01
k7 (Vmax,transport).... 1.5000E+00
k8 (KM, transport).... 2.9000E-04
k9 (Vmax tyrosinase)... 2.8600E+00
k10 Istore remove Tyr.. 2.5000E-02
k11 dopamine re-entry.. 1.0000E+00
k12 KI(Tyr) TH..... 5.0000E+01
k13 KM(DOPA) tyrosinase 2.2000E+01
k14 ROS DOPA pathway... 0.0000E+00
k6(k7-k11)/(k5+k11-k7). 5.3846E+00
Concentrations at end of phase 3 :
1.575E+02, 5.385E+00, 2.919E+02

Final concentrations:
1.575E+02, 5.385E+00, 2.919E+02

```

FIGURE 3.2: The experimental determined concentration values of constants k_1 - k_{14} presented in input file for Model 1 (left). The label "TH7-01" refers to the models run-id. The concentrations of each constant are the same for all three phases. These are changed later on. Summary of the compilation is presented in the column to the right.

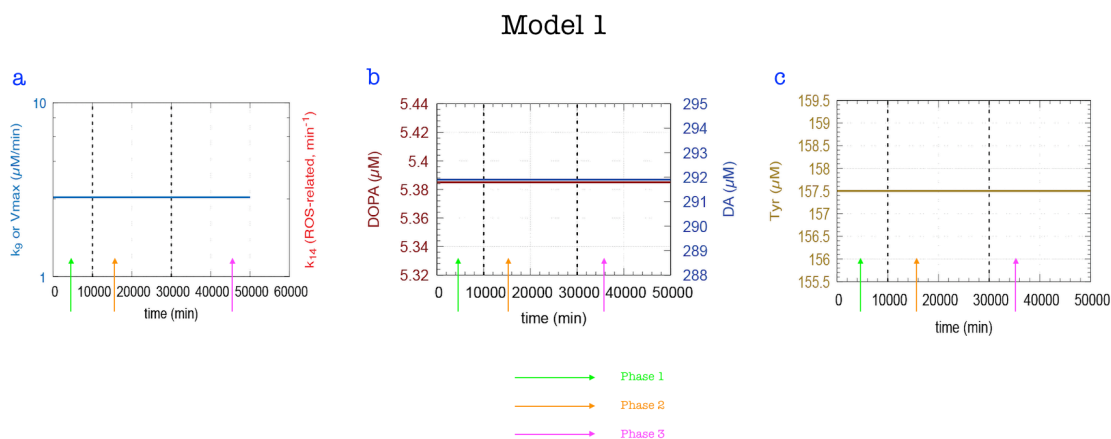


FIGURE 3.3: Graphic results when Model 1 was compiled. All constant values are the same for all three phases, as this model is used as a reference model. Phase 1, 2 and 3 are color coded with arrows. (a) k_9 values remains constant at around $5.00 \mu M$. (b) DA (blue) is unchanged at $292.00 \mu M$, and DOPA (red) around value $5.39 \mu M$ (c) Tyrosine is also unchanged around $157.50 \mu M$.

3.1.2 Regulation of Tyr, DOPA and DA by altering k_1

k_1 represents the flux (j_1) that is directly connected to Tyrosine in the reaction scheme.

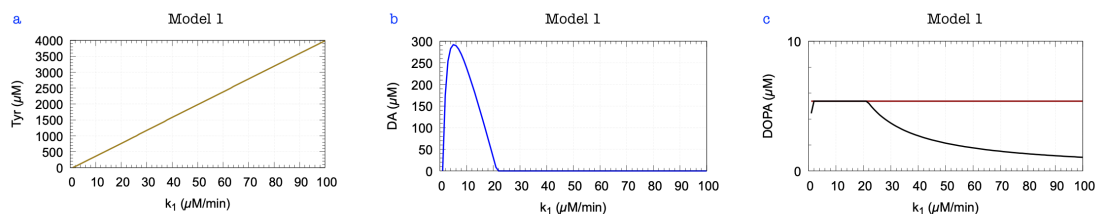


FIGURE 3.4: Results when k_1 was altered in Model 1. (a) Tyrosine levels (yellow) showed a steady, linear increase as higher k_1 values was applied. (b) Dopamine (blue) experienced a rapid increase, peaking at value $300 \mu M$, before decreasing at a high rate until k_1 equaled $20 \mu M/min$. (c) Steady-state value of DOPA (black) was reached until $k_1=20 \mu M/min$. DOPA set values (red) is here used as a constant.

Figure 3.4 presented an increasing concentration of Tyrosine as k_1 was increased. The flux is directly connected to the production of this Dopamine precursor, and would therefore with no doubt affect the concentration likewise.

However, the Dopamine and DOPA concentrations exhibited an interesting relationship. After upholding a constant and unchanging rate, the steady-state value of DOPA suddenly started dropping. Meanwhile, Dopamine concentrations encountered heightened levels, lowering at the approximately same rate before entering a constant concentration. Both graphs experienced a shift in concentration around $k_1=20 \mu M/min$. The change

in DOPA steady-state graph indicated that homeostasis was not maintained after this point. This phenomenon proved that overloading the inflow controller with excessive concentration values could not be accomplished without consequences. The cost of this action involved dysregulations in the internal stability.

3.1.3 Negative feedback mechanisms leads to accumulated levels of Dopamine

The enzyme Tyrosine Hydroxylase (TH) receives negative feedback signals from Dopamine (DA) through constant k_4 and from Tyrosine through constant k_{12} (Figure 3.1). Depicted feedback mechanism involving k_4 is also known as competitive inhibition. The inhibition term by Dopamine acts here directly on k_3 , the K_M -value of TH. A general representation of competitive inhibition is illustrated in Figure 3.5. No product is formed from EI as a consequence of the constructed enzyme-inhibitor complex (EI).

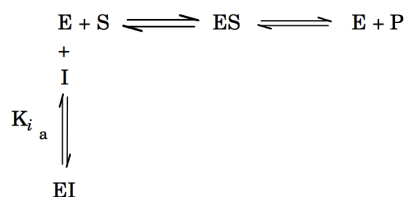


FIGURE 3.5: Competitive inhibition scheme [1]. The enzyme and substrate either forms the traditional enzyme-substrate complex (ES) or enzyme-inhibitor complex (EI). Latter reaction is reversible.

K_i represents the inhibition constant in given example. It is also known as an equilibrium constant. K_i can be expressed as a function of the inhibitor concentration, free enzyme concentration, and enzyme-inhibitor complex. The rapid equilibrium is presented in the equation:

$$K_i = \frac{[E][I]}{[EI]} \quad (3.5)$$

The competitive inhibition scheme in Figure [1] introduces the following equation:

$$[E]_{total} = [E]_{free} + [ES] + [EI] \quad (3.6)$$

Which in turn can be expressed through the Michaelis-Menten equation:

$$K_M = \frac{[E][S]}{[ES]} \quad (3.7)$$

After some readjustment of Equation 3.5 and Equation 3.7, we get an expression of v :

$$v = \frac{V_{max}[S]}{K_M[1 + \frac{[I]}{K_i}] + [S]} \quad (3.8)$$

Equation 3.8 illustrates how the velocity is determined and its relationship with V_{max} and K_M . A common feature of competitive inhibition is that the velocity is not affected because this type of inhibition can be completely overcome by high substrate concentrations [27].

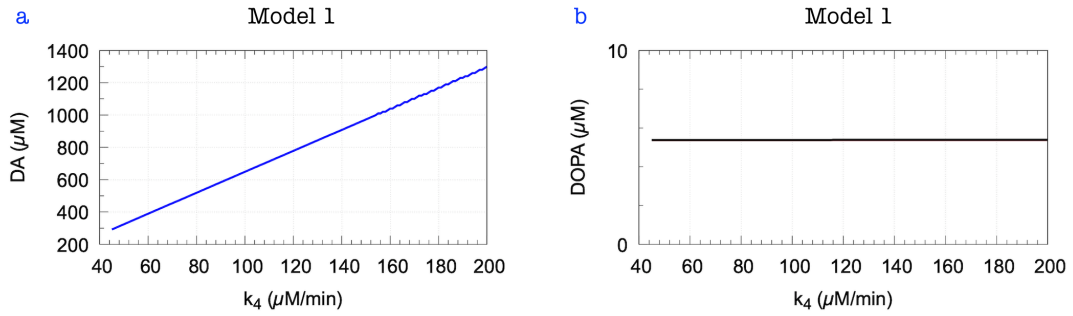


FIGURE 3.6: Results when k_4 (inhibition constant) was altered in Model 1. (a) Dopamine experienced a steady, linear increase, reaching values as far as 1300 μM when $k_4=200 \mu M/min$. (b) Steady-state values of DOPA remained unchanged throughout the reaction, implying preserved homeostasis.

Figure 3.6(a) showed that the implementation of higher constant values expressing negative feedback resulted in accumulated concentrations of Dopamine in the cell. $DOPA_{set}$ value (Figure 3.6(b)) remained unchanged and therefore homeostatically regulated. In conclusion, the k_4 constant played a significant role in maintaining homeostasis by increasing the DA concentration. This act of increase seemed to alter DOPA into achieving steady-state. It was clear that this feedback mechanism was an important contributor to the final outcome of Dopamine in the cell and thereby the regulation of DOPA.

The inhibition reaction gives us:

$$K_i = \frac{[E \cdot S][S]}{K_i} \quad (3.11)$$

By readjusting Equation 3.10 and Equation 3.11, we get an equation that features the velocity:

$$v = \frac{k_2 \cdot E_0}{1 + \frac{K_M}{[S]} + \frac{[S]}{K_i}} = \frac{V_{max} \cdot [S]}{K_M + [S] + \frac{[S]^2}{K_i}} \quad (3.12)$$

The simulations on constants k_4 and k_{12} resulted in increased Dopamine levels. The frequently wavering DOPA steady-state concentration (black) in Figure 3.7(b) suggested that homeostasis was not quite achieved. This event occurred even though Dopamine exhibited a heightened concentration outcome. In conclusion, DA was not able to homeostatically regulate DOPA for k_{12} as it did for k_4 .

Dopamine deficiency is seen as a consequence of aging as it is commonly found in elderly people [28]. The reason behind this is that aging is accompanied by profound changes in the brain's Dopamine system, and therefore highly affects cognitive function [29]. Deficiency results in loss of Dopamine production as well as loss of nerves to respond to DA release. Symptoms include muscle cramps, aches, stiffness in the muscles, loss of balance and mood swings. A Dopamine deficiency may be related to certain medical conditions such as depression and Parkinson's disease (PD). Dopamine production decreases gradually with age, which may be one reason why PD mainly occurs in older adults [30].

Oxidative stress is highly related to PD due to the fact that it plays an important role in the degeneration of dopaminergic neurons [31]. The phenomenon is activated by elevated levels of Reactive Oxygen Species (ROS) [32]. Inhibition of ROS accumulation in the cell could be accomplished by the regulation of DOPA. k_4 has so far proven itself as an effective agent on this matter, as it seemingly altered DOPA levels into homeostasis by increasing DA concentration (Figure 3.6). DOPA regulation is a source of reducing expression of oxidative stress [33]. k_4 can therefore serve its purpose as a treatment option for oxidative stress, which further reduces the risk of Dopamine deficiency and PD. The alteration of this constant can therefore through careful research potentially become a medical source for treating patients with Dopamine deficiency.

3.1.4 Broken homeostasis by the alteration of V_{max} of VAT2

The k_7 -constant represents the V_{max} value of the enzyme vesicular monoamine transporter 2 (VAT2). VAT2 is an integral membrane protein that carries out the transport of the monoamines, which in this case constitutes Dopamine [34]. Dopamine is translocated from cytosol across the vesicle membrane into the vesicle lumen following neurotransmitter biosynthesis.

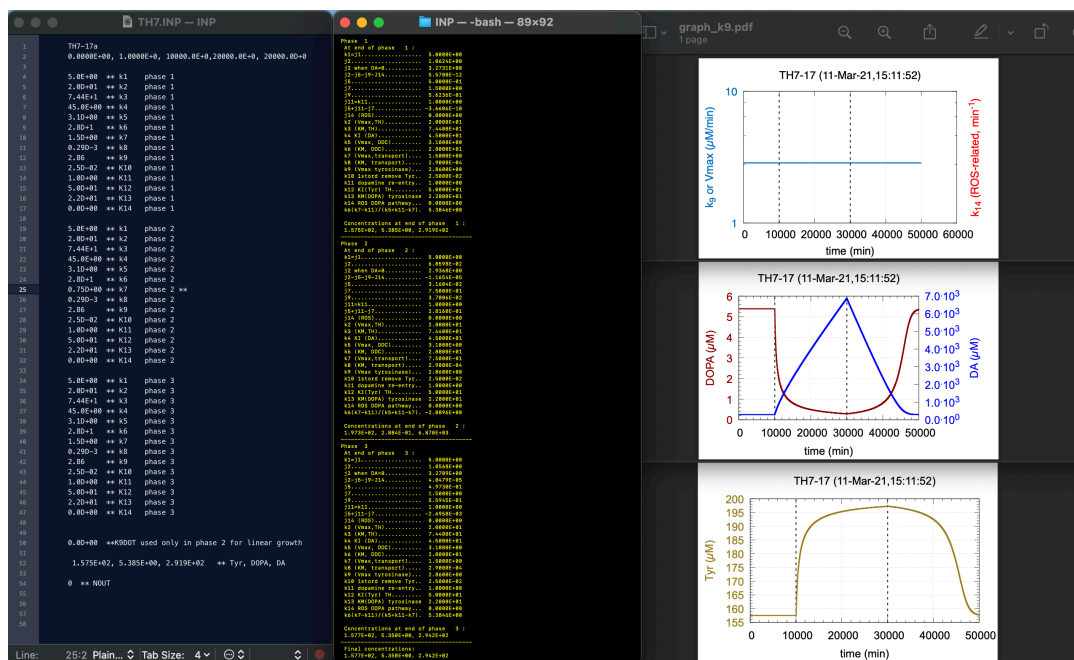


FIGURE 3.9: Results when the k_7 -constant was decreased by 50% ($k_7=0.75 \mu\text{M}$) in Model 1. DOPA levels were heavily decreased in phase 2. Meanwhile, Dopamine concentration were increased to an extreme extent, peaking at $7000 \mu\text{M}$. The graphs of all compounds had slow incline/decline in phase 3 as time went by. This slow uptake before reaching steady-state revealed that homeostasis was broken.

k_7 presented, as mentioned, an interesting outcome. Here, the homeostasis was broken when the constant value was reduced by 10% or more. Already at 25% reduction value, DOPA-levels started to decrease drastically in phase 2. However, DOPA-concentration had a slower increase per time unit in the 3rd phase unlike the other results. This exception became more prominent when k_7 was decreased even further by 50%, as seen in Figure 3.9. It had unusually difficulty in reaching steady-state. The results indicated that homeostasis was not preserved when the constant was altered to a certain extent.

Dopamine concentrations were severely increased compared to the other simulations. It's highest value peaked at $7000 \mu\text{M}$ when the k_7 -constant was decreased by 50% (Figure 3.9). Like the case of DOPA, the simulation showed slow increase per time unit in 3rd phase before reaching steady-state. This also happened when k-value was

decreased by 25% or more. In contrast, Dopamine levels started to drop when constant was increased by 10% or to a further point.

Tyrosine levels showed signs of delayed homeostasis regulation when exposed to a decreased k-value of 50% (Figure 3.9). The reaction needed abnormally long time (50 000 min) before the increased Tyrosine concentrations in the 3rd phase showed signs of adjusting back to normal values.

Decreasing the k_7 -constant would in this case equal decreasing V_{max} value of VAT2. The resulting reduction of DOPA-concentration could be explained by the fact that the upcoming vesicle loading process needed a longer time response to stabilize the accumulated levels of DA. As a consequence, large amounts of Dopamine were trapped inside the cell. The elevated concentrations of DA was a feedback response with the purpose of regulating DOPA back to steady-state. However, homeostasis was not achieved, which revealed that the cell was relatively fragile when exposed to altered k_7 -concentrations. DA was not able to regulate DOPA in this case.

k_7 is part of the DOPA set-point Equation 3.13, which explains why the constant played a significant role in regulating homeostasis.

$$DOPA_{set} = \frac{k_6 \cdot (k_7 - k_{11})}{k_5 + k_{11} - k_7} \quad (3.13)$$

By inserting the constant values for k_5 , k_6 and k_{11} (Figure 3.9), we get a function ($f(x)$) expressing change/increase in $DOPA_{set}$ as a function of k_7 :

$$f(x) = \frac{28 \cdot (x - 1)}{(4.1 - x)} \quad (3.14)$$

The exponential increase in DOPA set-point is further presented in Figure 3.10:

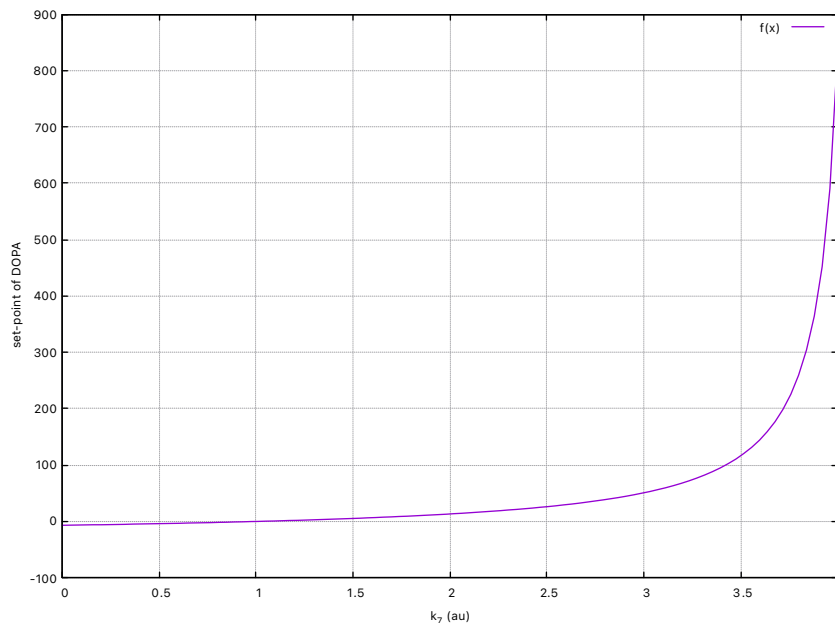


FIGURE 3.10: Exponential increase in DOPA set-point (Equation 3.14) as a function of k_7 . Values $k_5=3.1 \mu M$, $k_6=28.0 \mu M$ and $k_{11}=1.0 \mu M$ are inserted.

Figure 3.10 illustrates why homeostasis was broken when $k_7=0.75 \mu M$ was applied in phase 2 (Figure 3.9). At this point, set-point of DOPA reached $0 \mu M$.

Further experiments on the k_7 -constant were carried out to test whether or not the cell could adapt when two extreme constant-values were put together. A hypothesis was constructed on this matter:

Hypothesis 1. Unregulated levels of DOPA, Dopamine and Tyrosine in the cell due to increased/decreased constant value in phase 2 can be readjusted to homeostasis. This is completed by the application of the contrary increased/decreased constant value in phase 3.

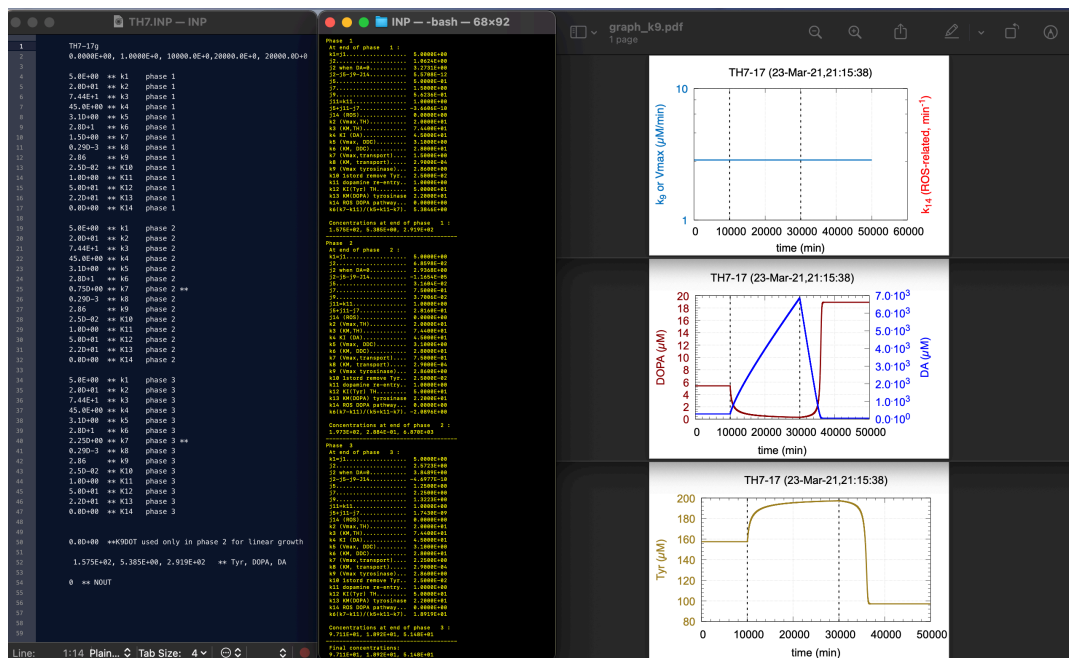


FIGURE 3.11: Results when $k_7=0.75 \mu\text{M}$ in phase 2 and $k_7=2.25 \mu\text{M}$ in phase 3. This ended in a quicker response time in contrast to when $k_7=0.75 \mu\text{M}$ only in phase 2.

The results of this experiment, presented in Figure 3.11, confirmed the stated hypothesis (Hypothesis 1). A low constant-value in phase 2 put together with a high constant-value in phase 3 gave, as mentioned, a quicker response time. Another prominent trait was how the values of DOPA, DA and Tyr became stabilized in the third phase. This stabilization was initiated by the changes in set-point (Figure 3.10).

Vesicular monoamine transporters are responsible for the packaging of neurotransmitters into synaptic vesicles [35]. The neurotransmitters include Dopamine, Norepinephrine, Epinephrine and Serotonin. The primary function is to segregate neurotransmitters within vesicles, but they can also translocate toxicants away from cytosolic sites of action. These roles of the enzyme are important in preventing oxidative stress. Methamphetamine is a highly addictive drug which is neurotoxic to Dopamine [35]. It destroys axon terminals by interfering with vesicular segregation and increasing Dopamine production. As a result, the amount of DA in cytosol is accumulated and the cell experiences oxidative stress. Vesicular transport keeps this reaction in check by sequestering excessive Dopamine. This action marks the importance of the VAT2 enzyme.

With this information at hand, we can safely confirm that k_7 (V_{max} of VAT2) plays an important role in the Dopamine pathway. It maintains homeostasis by regulating set-point of DOPA. DA is heavily increased in this regulation process.

3.1.5 Set-point changes results in preserved homeostasis

k_{11} denotes the re-entry of Dopamine into the cell. Changing this constant played a significant role on homeostasis preservation.

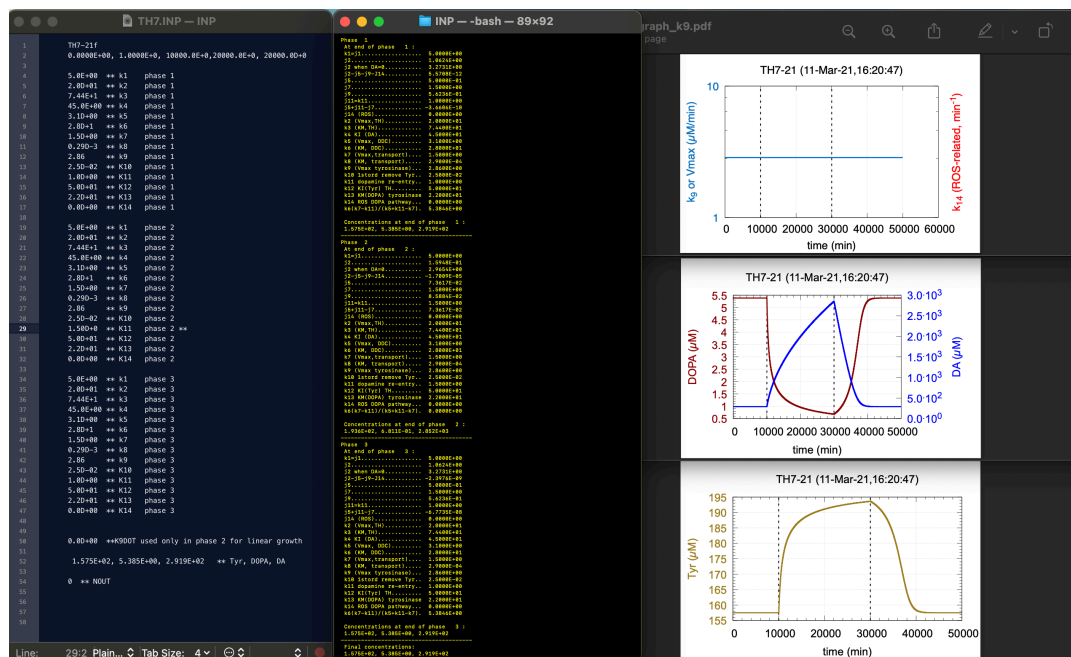


FIGURE 3.12: Results when the k_{11} -constant was increased by 50% ($k_{11}=1.5 \mu M$). DOPA levels became highly decreased in phase 2. Meanwhile, Dopamine concentrations experienced a towering high level around the same time interval. Tyrosine levels increased in the same phase, followed by a slow decline in phase 3. The time-slowness in phase 3 revealed that homeostasis was not maintained.

Struggles of upholding DOPA homeostasis became graphically visible in early stages when the constant concentrations was percentwise increased. Most prominent was the result of increase by 50%, shown in Figure 3.12. Here, DOPA in the 3rd phase required significant longer time (around 40 000 min) in reaching steady-state.

Extremely high concentration levels of Dopamine were a compelling result of this simulation, reaching as far as $3000 \mu M$ when k_{11} was increased by 50% (Figure 3.12). The same compilation also featured a longer time response in the 3rd phase. Steady-state of DOPA was not achieved until around 40 000 min.

Tyrosine concentrations also experienced difficulty in achieving homeostasis when k_{11} was percentwise increased. The higher the constant concentration, the longer it took for the reaction to reach steady-state in the phase 3.

k_{11} is, like k_7 , part of the DOPA set-point Equation 3.15. The equation was once again the source of DOPA regulation and homeostatic control. Constant values from Figure

3.12 were inserted into Equation 3.15. $F(x)$ expresses the changes in in $DOPA_{set}$ as a function of k_{11} :

$$DOPA_{set} = \frac{k_6 \cdot (k_7 - k_{11})}{k_5 + k_{11} - k_7} \quad (3.15)$$

$$f(x) = \frac{28 \cdot (1.5 - x)}{(x + 1.6)} \quad (3.16)$$

The decrease in DOPA set-point is further presented in Figure 3.13:

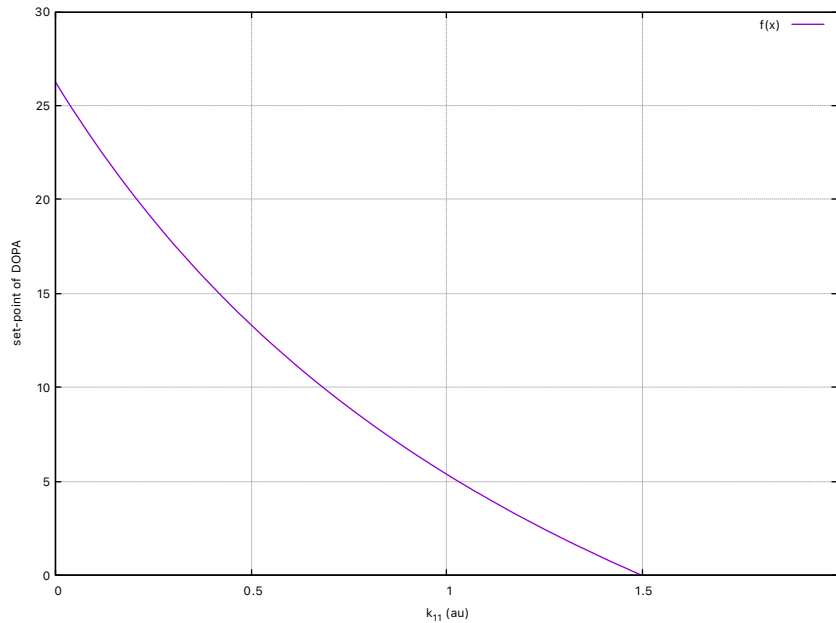


FIGURE 3.13: Decrease in DOPA set-point (Equation 3.16) as a function of k_{11} . Values $k_5=3.1 \mu M$, $k_6=28.0 \mu M$ and $k_7=1.5 \mu M$ are inserted.

Figure 3.13 illustrated an explanation to why we experienced broken homeostasis at $k_{11}=1.5 \mu M$. Set-point of DOPA had reached value $0 \mu M$ at this point. Homeostasis was not preserved as steady-state of DOPA could not be obtained.

The k_{11} -value is directly connected to cytosolic DA (Figure 3.1), which explains why the cell experiences higher concentrations of Dopamine when the constant is increased. Earlier simulations on constant k_7 (Figure 3.9) had similar results. DOPA homeostasis became unbalanced as a result of set-point changes.

It seemed convenient to test whether the earlier stated hypothesis (Hypothesis 1) could be strengthened in this case study. The same method was enforced using the concentration $k_{11}=1.5 \mu M$ in the second phase. This was the increased value that broke

homeostasis in the first place (Figure 3.12). k_{11} was set to $0.5 \mu M$ in the third phase. By doing this, it was assumed that DOPA would become homeostatically regulated.

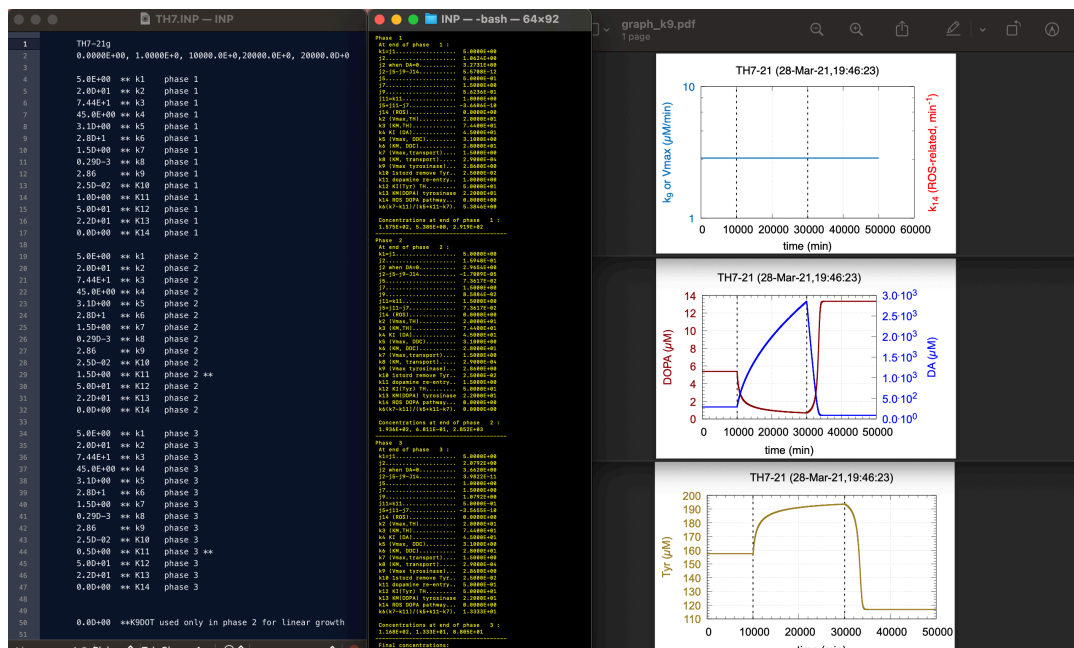


FIGURE 3.14: Results when Hypothesis 1 was applied in the goal of testing whether two contrast constant values would make the cell adjust itself into a more homeostatic environment. k_{11} was set to $1.5 \mu M$ in phase 2 and $0.5 \mu M$ in phase 3. DOPA, Dopamine and Tyrosine revealed a shorter time response in phase 3.

The results were as expected. The cell adjusted to homeostatic conditions in a quicker time response interval. This transpired around approximately 35 000 min. Hypothesis 1 was once again confirmed. Earlier simulation shown in Figure 3.12 required a bit more effort in achieving the same results (around 50 000 min). DA had a more rapid decrease in phase 3 in Figure 3.14 compared to Figure 3.12, which indicated that the Dopamine concentration had to be lowered as fast as possible in order for DOPA to achieve desired steady-state. However, for this to happen, the cell required heightened DA levels in phase 2. DOPA was once more regulated by increased values of DA. In conclusion, k_{11} had an important influence upon DOPA levels because of its appearance in the set-point equation (Equation 3.15).

$$\frac{d(DOPA)}{dt} = \frac{k_2 \cdot Tyr}{k_3 \left(1 + \frac{DA}{k_4}\right) \cdot \left(1 + \frac{DOPA}{k_{16}}\right) + Tyr} \cdot \left(\frac{k_{12}}{k_{12}} + Tyr\right) \quad (3.18)$$

$$- \frac{k_9 \cdot DOPA}{k_{13} + DOPA} - \frac{k_5 \cdot DOPA}{k_6 + DOPA} - k_{14} DOPA \quad (3.19)$$

$$- \frac{k_{15} \cdot DOPA}{k_{16} \left(1 + \frac{Tyr}{k_3}\right) + DOPA} \quad (3.20)$$

$$\frac{d(DA)}{dt} = \frac{k_5 \cdot DOPA}{k_6 + DOPA} - \frac{k_7 \cdot DA}{k_8 + DA} \quad (3.21)$$

3.2.1 Parkinson's Disease is highly connected to TH regulation

Tyrosine Hydroxylase exists in all dopaminergic cells as it catalyzes the formation of DOPA. The enzyme is a highly specific, non-heme iron, tetrahydrobiopterindependent protein. It catalyzes the conversion of Tyrosine to DOPA. TH is found in the neuroendocrine system, mainly in brain and chromaffin cells of adrenal medulla [36].

Parkinson's disease (PD) is known to be the most common neurodegenerative disorder. It affects more than 1% of the worldwide population over the age of 65 [37]. The loss of Dopamine in the striatum is a common feature seen in patients with PD. The neurotransmitter plays a significant role in brain function, and reduced levels are the main contributor to motor symptoms in PD. Causes of deficiency lies in the Dopamine signaling pathway, which includes synthesis, storage, release and recycling of Dopamine in the presynaptic terminal. It also includes the activation of pre- and post-synaptic receptors and downstream signaling cascades. Symptoms of PD include tremor, slowed movement, rigid muscles, impaired posture and speech changes. Deficiency in TH is a main contributor of PD, as it leads to deregulated Dopamine levels [37].

Restoration of Dopamine is seen upon as the main treatment option of preventing PD. This includes methods such as treatment with DOPA, DA agonists, inhibitors of DA metabolism or brain grafts with cells expressing a high level of TH.

3.2.2 Tyrosine Hydroxylase and its effect on maximum velocity

Noticeable changes were observed when k_2 was altered. The constant expresses V_{max} of the enzyme Tyrosine Hydroxylase (TH).

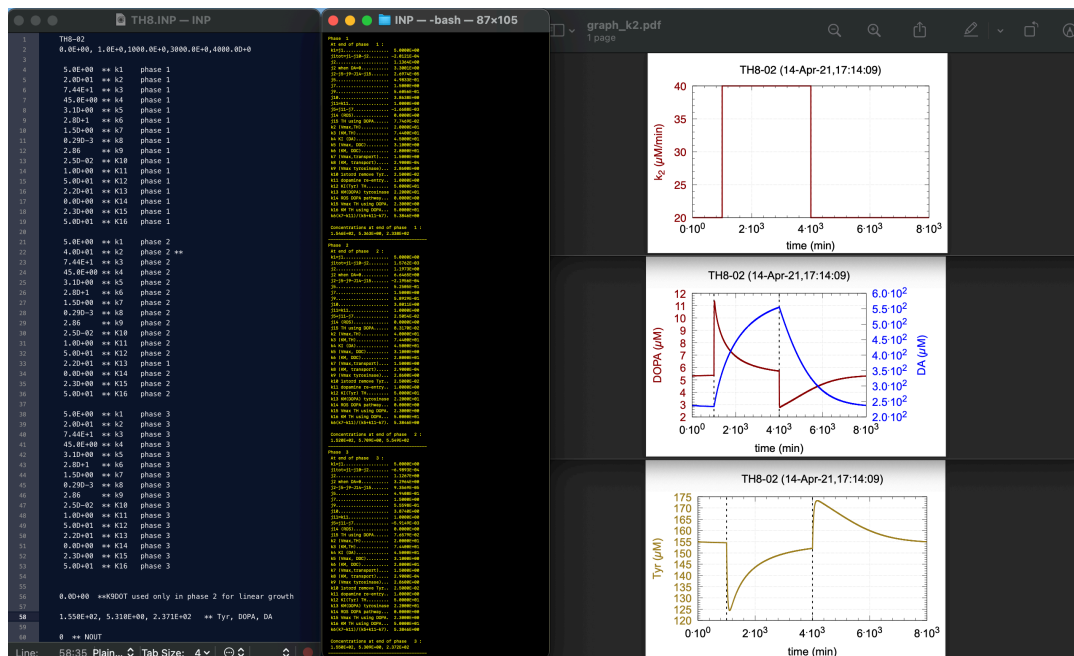


FIGURE 3.16: Results when V_{max}/k_2 had initial value of $k_2=20 \mu M$. The constant was changed to $k_2=40 \mu M$ in phase 2. DOPA levels had a slight increase in phase 2 before it became stabilized in phase 3. Both Dopamine and Tyrosine seemed to experience difficulties in achieving homeostasis in the third phase.

Tyrosine presented interesting results regarding the changes on k_2 . At first, the concentration decreased to $125 \mu M$ in the second phase. However, a surprising concentration increase was spotted in the third phase. This happened shortly after Tyrosine levels had reached start concentration in the second phase.

Dopamine levels were significantly affected by the increased constant values in Figure 3.16. The immediate increase of the neurotransmitter seen in phase 2 followed by the slow decrease in phase 3 indicated that homeostasis was broken. The cell clearly encountered struggles in regulating the concentration changes. This suggests that V_{max} -value of the j_2 -flux plays an important role in regulating this outcome.

3.2.3 DA regulates TH through competitive inhibition

Model 1 illustrated how competitive inhibition by TH (k_4) was a key factor in DOPA regulation. Tyrosine Hydroxylase is known to be the rate-limiting enzyme in the biosynthesis of Dopamine [38]. The mechanism enables DOPA to receive negative feedback from DA in order to achieve homeostasis. Simulations on Model 2 was completed in order to check how the addition of TH in the melanin pathway affected the outcome of DOPA and DA when k_4 was altered.

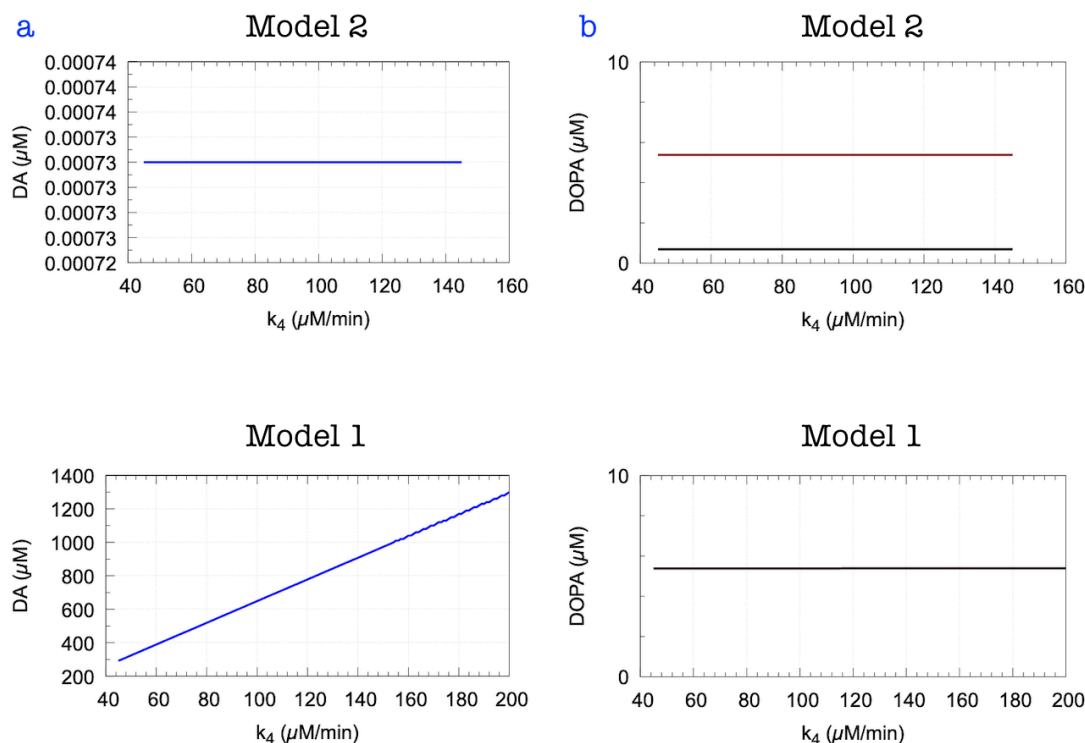


FIGURE 3.17: Comparison of Model 1 and Model 2 when k_4 was altered. The figure illustrates how TH-expression in the scheme of Model 2 overall affected the outcome of Tyr, DA and DOPA. (a) Model 1 showed a linear increase in DA and reached values up to $1400 \mu M$ at a relatively high rate. Meanwhile Model 2 had steady and low concentration values throughout the simulation ($0.00073 \mu M$). (b) DOPA steady-state and set-point value was maintained at a constant level for both Model 1 and Model 2.

Model 2 had an interesting result compared to Model 1 with respect to k_4 . For instance, the proportional increase in DA in Model 1 (Bottom in Figure 3.17(a)) was now replaced by steady and constant values in Model 2. The inclusion of TH through constants k_{15} and k_{16} altered DA levels into a constant value. Steady-state values of DOPA (black) in Model 1 (Figure 3.17(b)) was achieved at a lower concentration compared to Model 2. DOPA was homeostatically regulated in both simulations as its levels remained unchanged throughout the reaction.

The increase of k_4 seemed to have very low impact on DA when TH was expressed in the neuromelanin pathway as well (Model 2). An explanation of this could be that the reaction probably favoured one turnover reaction over another. The first alternative route is the catalyzation of Tyr and the second path is the catalyzation of DOPA into Dopaquinone. The unchanged DA levels in Figure 3.17(a) could serve as a confirmation that the reaction favoured the turnover of DOPA in the melanin pathway. Nevertheless, since the simulation does not reflect the outcome of melanin, we can not present this as a reliable hypothesis.

DA has earlier proven to bind to TH with high affinity. Previous work revealed that TH contains a single high-affinity Dopamine-binding site. Studies obtained from an article published in 2008 stated that there existed two distinct Dopamine-binding sites in TH [39]. It was further proven that they represented a high-affinity binding site and a low-affinity binding site.

The low-affinity site seemed to play a major role in regulation of TH. When cytosolic Dopamine levels increase, Dopamine react by binding itself to the low-affinity site to inhibit TH activity. This response works as a prevention mechanism to reduce further accumulation of DA in the cytosol. Accumulation of cytosolic catecholamines has been hypothesised to contribute to the pathogenesis of Parkinson's disease [11]. Therefore, we can expect that the low-affinity Dopamine-binding site has a potential protective function. Its modulation of TH activity prevents cytosolic accumulation and possible neurological diseases.

The two affinity regulated binding-sites of TH can be an explanation to why DA levels were unaffected in Model 2 (Figure 3.17(a)). The presence of TH in two places could influence DA into binding to the low-affinity site of TH (k_4). Further formation of DA is either lowered or inhibited as a result. Figure 3.17(b) also proved that DOPA reached steady-state at a lower concentration in Model 2 than Model 1. The lowered steady-state values of DOPA seemed to be a cause of regulated DA levels, which once again confirms that DA is a homeostatic regulator of DOPA.

A research article from 1998 confirmed that Dopamine covalently modifies and inactivates TH through negative feedback [40]. This process happens in the presence of the melanin biosynthetic enzyme Tyrosinase. Dopamine can be oxidized to form Dopamine quinone, a reactive version that are able to modify cellular macromolecules including protein and DNA. Studies presented that the formation of Dopamine quinone was enhanced by the activity of Tyrosinase, which in turn covalently modified and inactivated TH. DOPA also contributed to inactivation of TH under these conditions.

The results in Figure 3.17 confirms this study, and also provides the suggestion that Tyrosinase could serve as a key regulator in TH expression.

3.2.4 TH alters V_{max} of VAT2 into achieving homeostatic control

Earlier studies on k_7 (Figure 3.9) showed that both Tyrosine and Dopamine had a drastic increase in concentration when lower k_7 -values were applied. It was further proven that the simulations on this constant presented reactions that performed poorly in maintaining homeostasis. However, simulations on Model 2 showed different results.

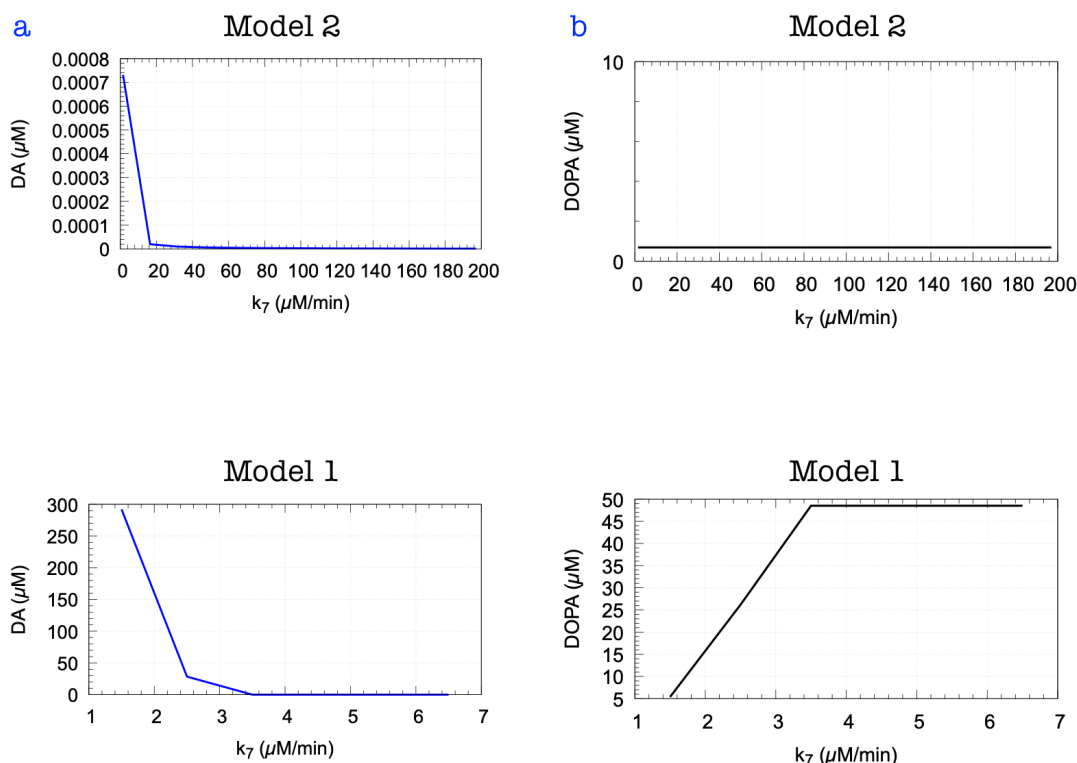


FIGURE 3.18: Comparison of Model 2 and Model 1 when k_7 (V_{max} of VAT2) was altered. (a) DA decreased in both simulations. However, Model 2 required application of way higher k_7 -concentrations to experience even a slight decrease in DA outcome. (b) DOPA had earlier expressed unregulated homeostasis as a result of changed steady-state values in Model 1. Model 2 showed results that now was homeostatically regulated now that a new behaviour of TH was introduced. DOPA concentration remained stabilized and unchanged.

The simulations on Model 1 and Model 2 in Figure 3.18 made it clear that DOPA was regulated by DA. Model 1 revealed this pattern by illustrating that the DOPA values (Bottom of Figure 3.18(b)) were returning to a steady-state around $k_7=3.5 \mu M$. Meanwhile, DA (Bottom of Figure 3.18(b)) exhibited a drastic decrease in values that eventually aligned its stabilization to constant levels at the same point as DOPA. Model 2 illustrated unchanged and constant values of DOPA, which expressed that steady-state was immediately reached. This pattern revealed that homeostasis was maintained in the presence of TH turnover of DOPA and Tyr. The same response was featured when Model 1 and Model 2 were compared on their influence on k_4 (Figure 3.17).

TH-expression proved once more to have a large impact upon final concentrations of mainly DOPA and DA. DOPA was again homeostatically regulated in Model 2 as a result of lower amounts of DA in the cell. The lower range of DA values in Model 2 ($0 \mu M - 0.0008 \mu M$) suggested that VAT2 did not favour DOPA formation by the presence of TH-turnover of both Tyrosine and DOPA. Nevertheless, homeostasis was maintained even though the cell expressed extremely low values of DA.

A study evaluating effects of pedunculo pontine nucleus (PPN) in TH, VAT2 and dopamine transporter (DAT) revealed that higher TH levels could stimulate Dopamine synthesis [41]. Dopamine is known as a highly reactive molecule and has a high tendency to form reactive oxygen species (ROS). This happens through its metabolism in the cytosol. The enzyme VAT2 contributes to vesicular packaging of Dopamine, which in turn prevents the harmful oxidation process. The article further discussed how decrease of VAT2 provided major issues for a dopaminergic cell. Lowered amounts of VAT2 mRNA expression led to alterations in Dopamine vesicular storage, which could be potentially toxic to the cell. VAT2 levels proved to be very important for dopaminergic functioning. It was concluded through this study that a possible oxidative stress environment favored the alteration in mRNA expression of several proteins (TH, VAT2, DAT) responsible for dopaminergic homeostasis.

The simulations in this subsection (Figure 3.18) signified that TH-expression regulated VAT2 in a way that resulted in DOPA becoming homeostatically controlled. This happened accordingly to Dopamine levels becoming severely reduced. The study presented in the paragraph above provided the suggestion that TH and VAT2 could be activated as a response to oxidative stress. The doubled turnover of TH suppressed the oxidative stress by lowering the DA concentration. VAT2 contributed as well by assisting DOPA into an instant steady-state to preserve homeostasis.

3.2.5 DOPA is not homeostatically regulated by the presence of TH when k_{11} is altered

Earlier simulations on Model 1 revealed that the constant experienced difficulties in upholding homeostasis when exposed to increased values of k_{11} . The constant represents the inflow of Dopamine from the synaptic cleft back into the cell. It seemed fit to test whether the new turnover function of TH presented in Model 2 gave a different result.

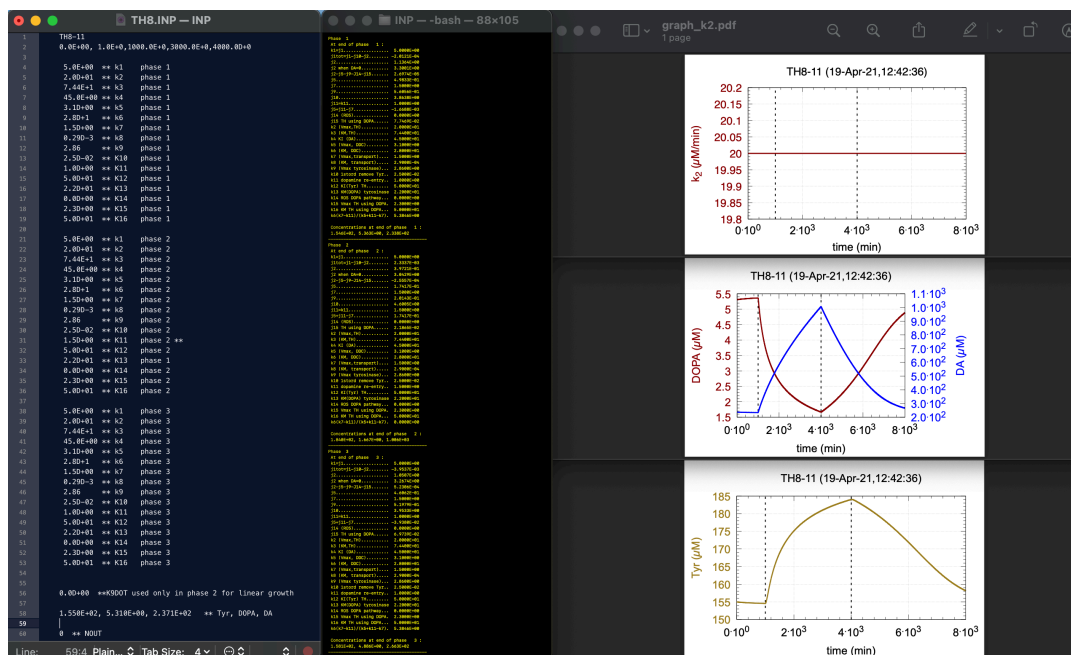


FIGURE 3.19: Results on Model 2 when k_{11} was increased by 50% like in Figure 3.12 (Model 1). The concentration value was set to $k_{11}=1.5 \mu M$ in phase 2. Dopamine and Tyrosine were both heavily increased in the second phase and decreased in phase 3. DOPA levels sunk in phase 2 followed by a shift in phase 3.

Figure 3.19 showed that DOPA, Dopamine and Tyrosine had problems in readjusting to homeostasis. This was illustrated by the slow uptake in concentration in the third phase. The simulation on Model 1 (Figure 3.9) did not reach steady-state until 5000 minutes had passed. Far more time had gone by (8000 min) in in experiments done on Model 2 (Figure 3.19) before the reaction even showed signs on returning to such conditions. The highest concentrations of DOPA, Dopamine and Tyrosine in last mentioned simulation were $950 \mu M$, $1000 \mu M$ and $185 \mu M$. These values were way lower than the concentrations presented in Model 1 ($6500 \mu M$, $7000 \mu M$ and $195 \mu M$).

So far we know that the inclusion of constants k_{15} and k_{16} , also known as the expression of TH turnover of DOPA, impacted the reaction by slowing down the reaction time. The overall concentration of DOPA, DA and Tyr had decreased as well. This occurred when Model 2 was compared to the results of Model 1 (Figure 3.9). A possible explanation of this phenomenon could be that presence of TH in two situations favours one TH-turnover over another. In this case, the turnover of DOPA (melanin pathway) seemed to be the preferred reaction path.

The Dopamine transporter (DAT) is a transmembrane-spanning protein. It is responsible for transporting DA out of the synaptic cleft of dopaminergic neurons. DAT expression declines in substantia nigra neurons due to aging [42]. k_{11} represents the function of DAT in Model 2 (Figure 3.15).

The Dopamine transporter regulates Dopamine levels in the cell. Dysfunction of DAT has proven to be a hallmark of Parkinson's Disease (PD), suggesting that Dopamine systems are deregulated in PD [43]. The transporter is also often the main target of antidepressants and drugs used for attention-deficit hyperactivity disorder therapies. This is because dysregulated DAT activity is often associated with neurological disorders.

In conclusion, the simulations on the k_{11} -constant representing the re-entry of DA proved that DAT was an important regulator in the dopaminergic cell. In this case, another function of TH illuminated a weak spot of the cell rather than a strengthened regulation of DOPA. The two turnover functions of TH seemed to alter the DAT in a way that delayed homeostatic regulation even further than when TH only catalyzed the turnover of Tyr (k_4). These results marked the importance of how re-entry of Dopamine into the cell affected the cell's ability to maintain homeostasis. A case of deregulation in DAT could involve consequences like symptoms of PD.

3.3 An overview scheme

This section presents an extended reaction scheme of Dopamine formation in vesicle pool, its path through the nerve impulse and lastly its release in synaptic cleft. The negative feedback reaction via auto-receptors is included. This reaction is carried from Dopamine in the synaptic cleft and affects Tyrosine Hydroxylase. New changes include the addition of the constants k_{17} - k_{21} (Figure 2.1) and the flux j_{11} , which is dependant on the concentration of DA in the synaptic cleft. DA is now homeostatically regulating DOPA both inside the cell through competitive inhibition (k_4) and outside in the synaptic cleft via D₂ autoreceptors (k_{20}). In this section we will take a closer look upon the negative feedback mechanisms in a broader view of the scheme. We will also shortly review what happens to Dopamine levels in the vesicle and synaptic cleft on constants k_7 and k_{11} .

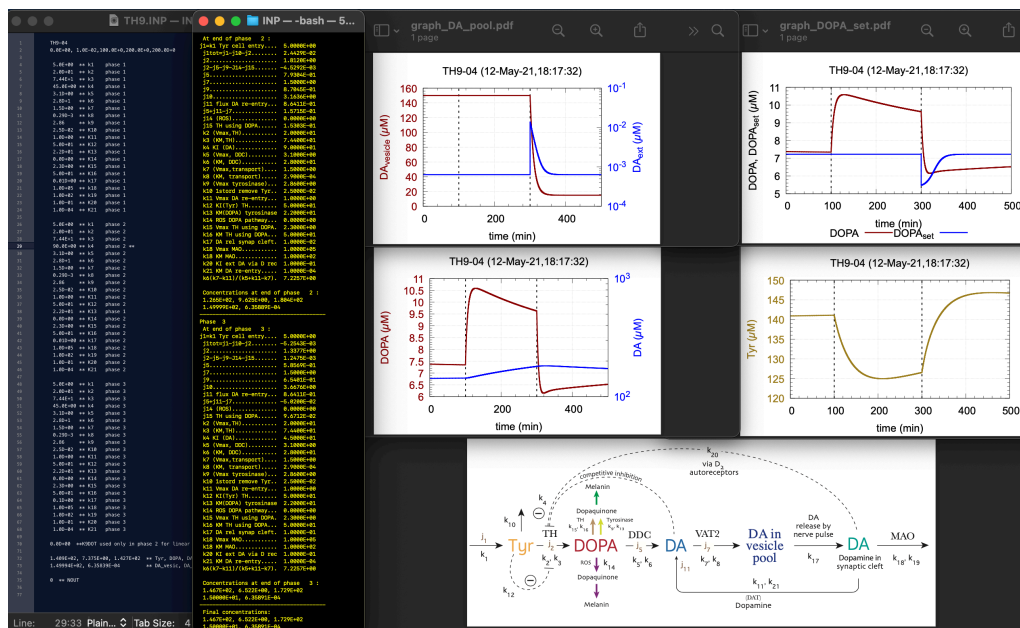


FIGURE 3.21: Results on Model 3 when k_4 was increased to $90 \mu\text{M}$ in phase 2. A drastic increase of DOPA occurred in phase 2 as DA levels slightly shifted to higher values in the same time interval. Both DOPA and DA in the cytosol encountered slightly difficulties in becoming stabilized, unlike external DA (DA_{ext}) and DA in the vesicle ($DA_{vesicle}$) who both eventually reached steady-state in phase 3. Tyrosine concentration decreased in phase 2, but its levels quickly accumulated in the last phase.

The results presented in Figure 3.21 showed that increase of k_4 had the most impact upon DOPA expression in the broader reaction presented in Model 3. Dopamine in the synaptic cleft (DA_{ext}) shifted slightly into phase 3, but became stabilized quickly. The vesicular DA dropped a lot. However, it was clear that the inhibition constant mainly focused on its negative feedback towards TH in the purpose of regulating DOPA.

The D2-autoreceptors play an essential role in regulating the activity of Dopamine neurons. They also control the synthesis, release and uptake of DA [44]. The autoreceptors are found at somatodendritic and axonal sites. Their main function is regulating the firing patterns of Dopamine neurons. The amount and timing of DA released are strictly controlled by the receptors. Alterations in the expression of autoreceptors are in many cases looked upon as a contributor to Parkinson's, schizophrenia, drug addiction and attention deficit hyperactivity disorder (ADHD). This section mainly focuses on how terminal D2-receptors change DA transmission through the inhibition of TH.

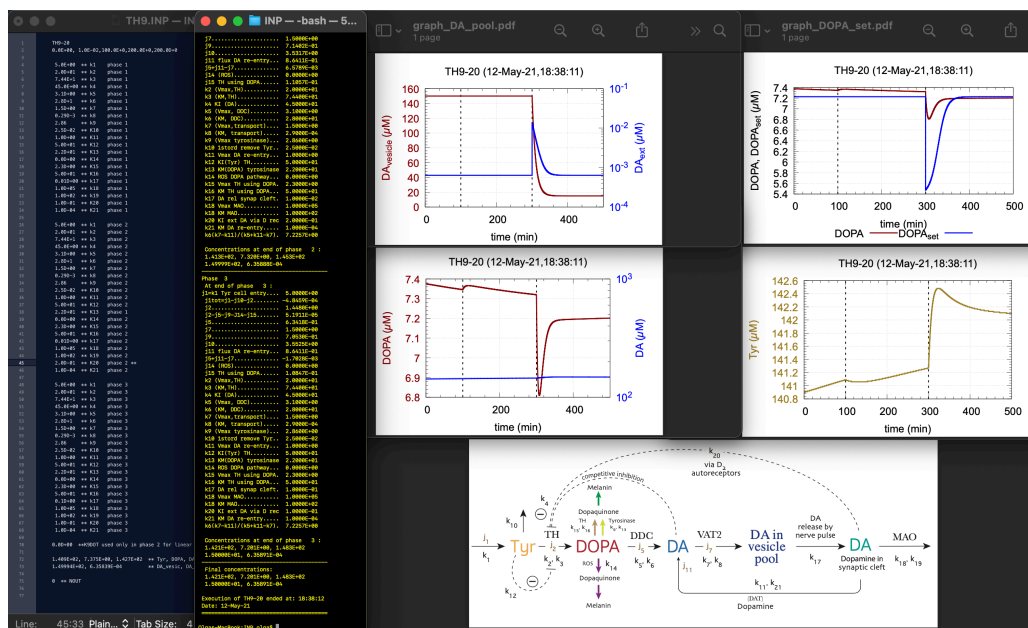


FIGURE 3.22: This figure illustrated what happened when k_{20} was changed to $0.2 \mu\text{M}$ in phase 2. Interestingly, DOPA concentrations were decreased throughout all three phases at the same time as the amount of DA in cytosol expressed almost unchanged values. DOPA values were almost completely aligned with set-values (DOPA_{set}) in the third phase, implying that homeostasis was maintained. Meanwhile, Tyrosine levels had an increase in phase 3.

The increase of k_{20} resulted mainly in heavily declined levels of DA in the vesicle. This phenomenon is scientifically proven in a study from 2014 on TH and its relation to D2-receptors [44]. Down-regulation of TH was claimed to be followed by prolonged auto-receptor activation, which in turn lead to reductions of Dopamine in the vesicle filling process. In addition it supposedly altered the distribution and expression of VAT2, which will be further investigated in the next section.

The D2-receptors are easily altered by drugs. Prolonged activation of these may occur by either low frequency electrical stimulation or by exogenous application of DA [44]. These processes drives long-term depression at somatodendritic Dopamine synapses. As a result, there is a high chance of firing processes taking place in Dopamine neurons. High exposure to drugs will in conclusion alter the cells ability to regulate the activity of DA. A single exposure of cocaine can dynamically regulate the somatodendritic synapses.

DA receptor agonists are also regarded as a medical treatment option. These receptors are used as combination therapy together with DOPA to retard the development of motor complications in advanced stages of PD [45]. They appear to direct stimulation of both presynaptic and postsynaptic receptors. However, the side effects of this treatment option are not studied enough, and may therefore be slightly less potent medicine than DOPA. It is also predicted that they can be poorly tolerated by older PD patients.

The D2 autoreceptors (k_{20}) seemed to mainly influence DOPA expression. This phenomenon was also seen in the case of inhibition by k_4 (Figure 3.21). However, homeostasis was not maintained in this simulation as DOPA levels did not reach steady-state. The results regarding k_{20} indicated that the cell was able to withstand elevated expression of negative feedback via the D2 autoreceptors.

3.3.2 VAT2 has a heavy impact upon DA in the vesicle pool

A simulation was created to check how the alteration of V_{max} of the enzyme VAT2 impacted the external DA and Dopamine in the vesicle loading process.

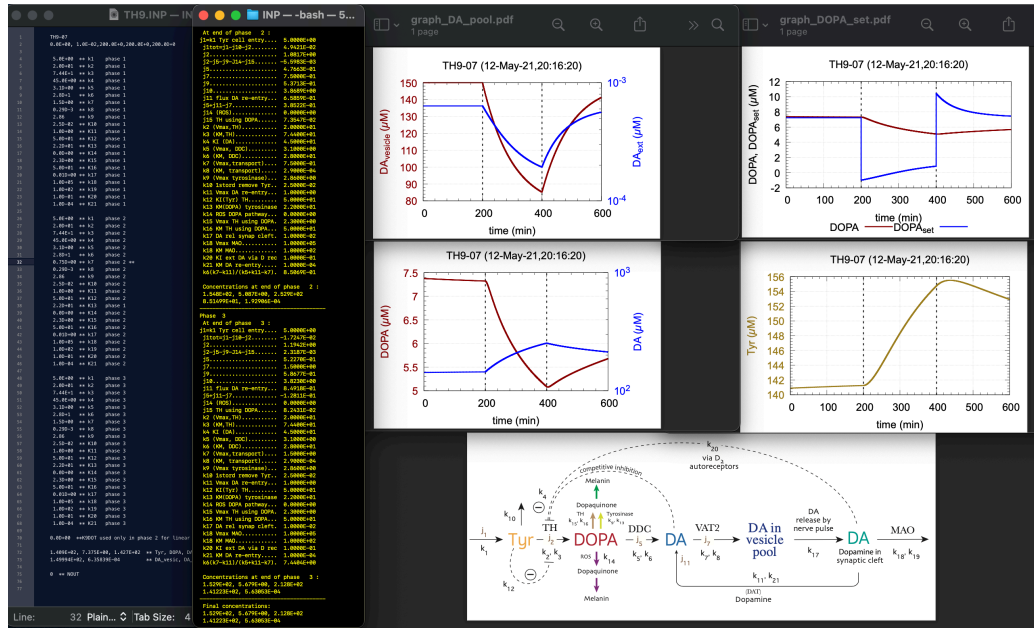


FIGURE 3.23: The alteration of V_{max} of VAT2. $k_7=0.75 \mu M$ was applied in the second phase. The DA-levels in the vesicle ($DA_{vesicle}$) and in the synaptic cleft (DA_{ext}) was instantly decreased throughout this phase and encountered struggles in returning to set-point in the third phase.

Earlier simulations regarding Model 1 presented that DOPA and DA had trouble upholding homeostasis when accompanied with decreased k_7 -values (Figure 3.9). The same was illustrated in Figure 3.23. The graph comparing DOPA with DA in cytosol showed once again that DOPA encountered struggles in upholding homeostasis, as the levels kept decreasing in the third phase in an uncertain prospect of reaching steady-state. Likewise, $DOPA_{set}$ -value was adjusted very slowly in the last phase when aligned with DOPA outcome. DA in the vesicle and synaptic cleft were both heavily decreased in phase 2. They did not manage to become stabilized in the third phase as well. Deregulation of enzyme VAT2 did not favour homeostasis as the process resulted in heavily

decreased levels of DA in the vesicle and external environment. Meanwhile, amounts of DA were accumulated in the cytosol.

3.3.3 A broader view of the inflow of DA

k_{11} has so far been the constant representing the inflow of DA. However, Model 3 (Figure 3.20) shows a inflow that is now replaced by the j_{11} -flux. k_{11} and k_{21} are at the same time depicted as V_{max} and K_m , and regulates the inflow of DA from the Dopamine in the synaptic cleft. A simulation on Model 3 was presented to show how this restructure affected the overall reaction.

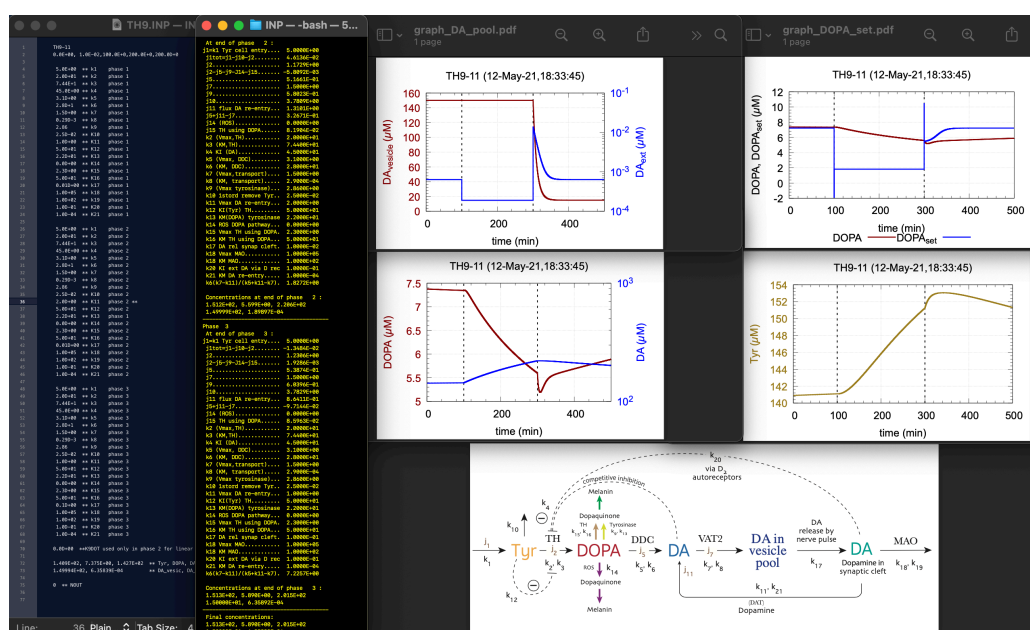


FIGURE 3.24: Results when k_{11} was changed from $1.0 \mu M$ to $2.0 \mu M$ in Model 3. The increase of inflow resulted in wavering levels of $DOPA_{set}$ throughout phase 1 and 2, followed by a slow regulation into steady-state in phase 3. DOPA concentration was decreased during phase 2 and encountered struggles in stabilizing in phase 3. External DA shifted to lowered values in phase 2, but stabilized in phase 3. Tyrosine levels accumulated throughout the same time period, especially in phase 2.

Earlier simulations on Model 1 and 2 exemplified how k_{11} played an important role in DOPA regulation. The cell revealed to be rather fragile when exposed to increased values of this constant as it was not able to maintain homeostasis. In the overall scheme represented by Model 3, the alteration of k_{11} did not seem to have a heavy impact upon DA in the synaptic cleft. Vesicular DA experienced its characteristic drop in phase 3, which also happened in Figure 3.22 and Figure 3.21.

Figure 3.24 suggested that $DOPA_{set}$ -point was altered by other parameters. Rheostasis is the term that elaborates this phenomenon pointing to the fact that the set-points

of homeostatic controllers may not be static, but instead change with environmental conditions [46].

3.4 DOPA as a treatment method

Treatment of Parkinson's Disease can be accomplished by L-DOPA medication [26]. Model 4 presents a new and external source of DOPA. The phenomenon is expressed by constant k_{22} and functions as a continuous DOPA medication. The constant values are the same as for the other models (Figure 2.1), with the additional value of $k_{22}=0.0 \mu M$, which is altered consequently in the subsections.

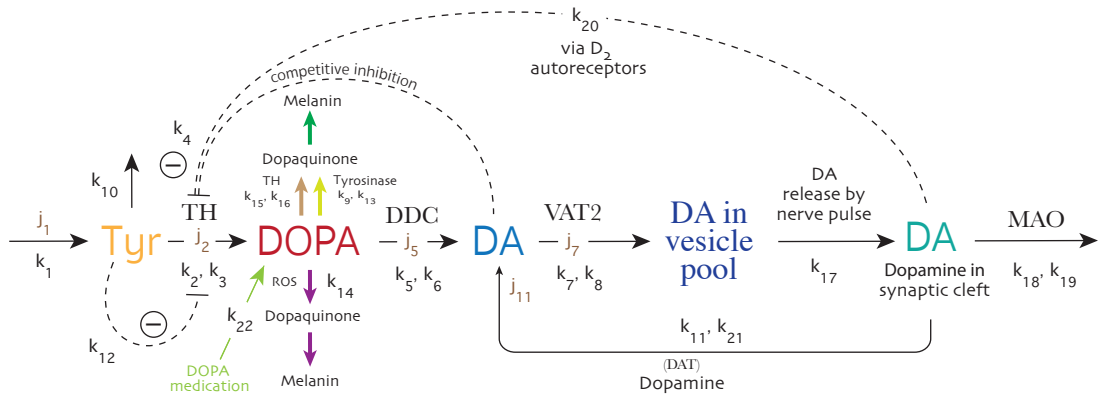


FIGURE 3.25: Reaction scheme for Model 4. Rate constant k_{22} represents an additional inflow of DOPA from an external source (green).

Rate equation of DOPA is presented in Equation 3.23:

$$\frac{d(DOPA)}{dt} = k_{22} + \frac{k_2 \cdot Tyr}{k_3 \left(1 + \frac{DA}{k_4}\right) + Tyr} \cdot \frac{k_{12}}{k_{12} + Tyr} - \frac{k_9 \cdot DOPA}{k_{13} + DOPA} - \frac{k_5 \cdot DOPA}{k_6 + DOPA} - k_{14} \cdot DOPA \quad (3.23)$$

3.4.1 DA restores DOPA homeostasis

A simulation on Model 4 was completed in order to check how the external inflow of DOPA through k_{22} could influence the cells regulation of homeostasis.

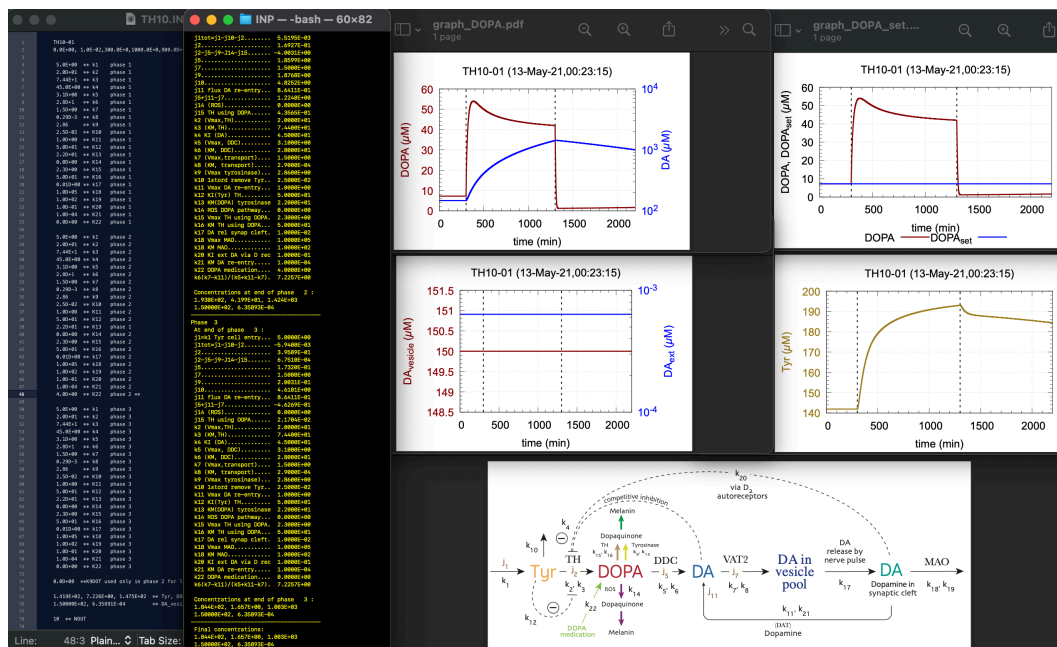


FIGURE 3.26: Results on Model 4 when k_{22} was changed to $2 \mu\text{M}$ in phase 2, expressing a continuous flow of DOPA into the reaction. Dopamine levels were increased in phase 2 as a result, which enabled DOPA to become homeostatically regulated. This event occurred in phase 3, and is confirmed by the steady values of $DOPA_{set}$.

Figure 3.26 presented results that illustrated how DOPA homeostasis was restored by the increase of DA values. Tyrosine decreased during phase 2 as a result of the increased compensatory flux j_2 in the purpose of opposing the perturbation. This outcome confirms that DOPA medication is a theoretically reliable source of treatment, as it inhibits deficiency of Dopamine and also regulate DOPA into steady-state to preserve a stable internal environment.

3.4.2 DOPA regulates oxidative stress

Parkinson's Disease is found to be a result of increased oxidative stress [31]. Accumulation of Reactive Oxygen Species in the cell is the main contributor to this phenomenon [32]. DOPA regulation is seen upon as a treatment method as a way of decreasing oxidative stress. This subsection presents a simulation where the ROS-constant (k_{14}) is increased and accompanied by the influence of a high external DOPA-flux (k_{22}).

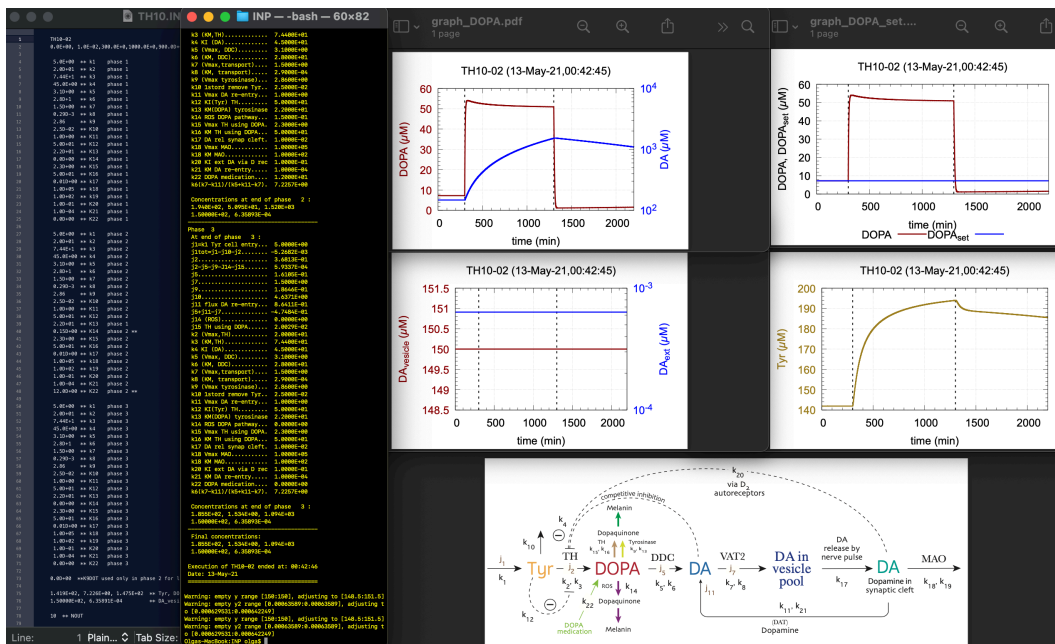


FIGURE 3.27: Results on Model 4 when $k_{22}=12 \mu M$ and $k_{14}=0.15 \mu M$ in phase 2. Dopamine levels were increased, which in turn restored DOPA homeostasis.

The external DOPA treatment method proved once more to be a successful tool in the aim of achieving internal DOPA homeostasis. This was yet again performed as a result of accumulated Dopamine levels.

3.5 MATLAB calculations

Values from Model 3 was in this section inserted into MATLAB. The intention was to confirm the results already illustrated by the Fortran model. The same constant values were applied in the MATLAB calculations, only these results presented the change in phase 2 of the model made in Fortran. The simulations altering constants k_4 and k_7 were used as models for comparison:

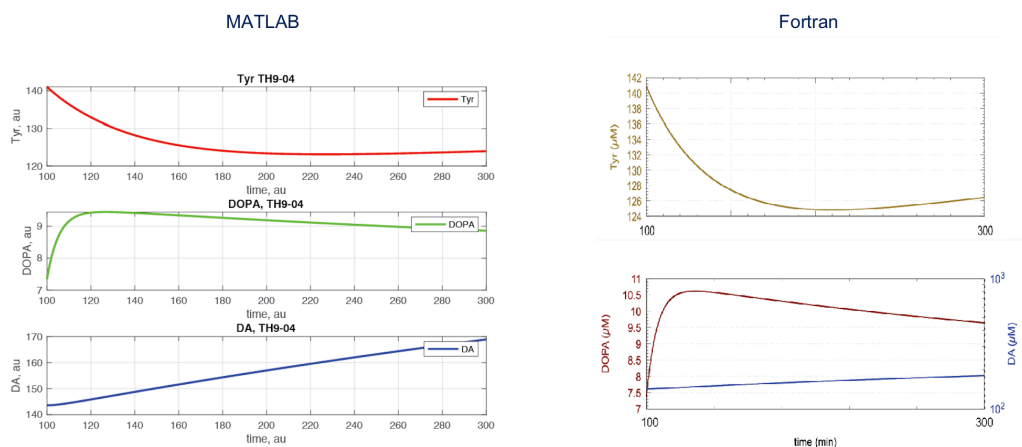


FIGURE 3.28: Comparison of MATLAB and Fortran results on k_4 with time interval $t=[100,300]$ (phase 2 in Fortran). Tyrosine decreased during this time period. DOPA was first heavily increased, and experienced a slow decline in concentration levels after 120 min. DA increased linearly.

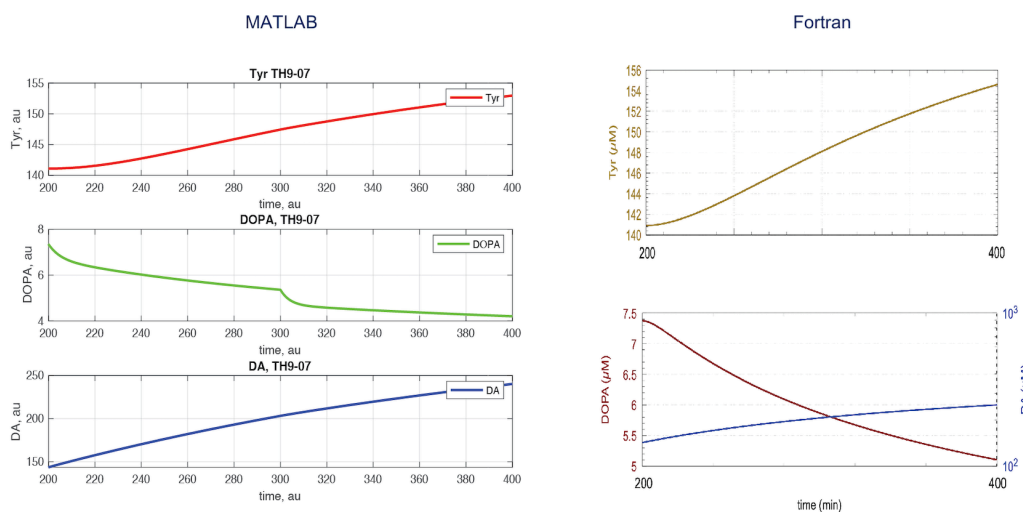


FIGURE 3.29: Comparison of MATLAB and Fortran results on k_7 with time interval $t=[200,400]$ (phase 2 in Fortran). Tyrosine increased throughout the reaction. DOPA experienced a decrease. Lastly, DA levels were increased linearly.

In conclusion, MATLAB provided results that were reassuring compared to the Fortran simulations.

3.6 Conclusion

The simulations carried out on models 1-4 signified the importance of DOPA regulation. Negative feedback mechanisms in the form of competitive inhibition, substrate inhibition and inhibition by autoreceptors proved to be important methods that ensured

that homeostasis was maintained. Disturbances in homeostasis occurred when constant values were increased/decreased to certain extent where DOPA struggled in reaching steady-state. Among these were the regulation of V_{max} -value of VAT2 and the flux (k_{11}) in Model 1. However, these results could be altered to achieve homeostasis by the application of compensatory values in the third phase. DOPA reached steady-state much quicker as a result of these set-point changes.

Another way of ensuring steady-state values of DOPA was the inclusion of Tyrosine Hydroxylase (TH) in the melanin pathway, now assuring that Tyrosine catalyzed both DOPA and Tyrosine. An exception was when the flux k_{11} was treated in this manner, which did not favour homeostasis, suggesting that TH had an inhibitory effect on the dopamine transporter (DAT). Loss of Dopamine is highly related to several neurodegenerative disorders such as Parkinson's Disease, and is also seen to be a result of aging. Restoration of Dopamine by DOPA medication is seen upon as a main treatment of these disorders. Dopamine regulation of DOPA proved through the simulations in the thesis to be an effective regulation tool of preserving homeostasis. Dopamine are in these cases restored to its desired levels and oxidative stress is inhibited. Evidence of successful DOPA treatment by continuous medication was presented through simulations on Model 4. The only remaining way of confirming these treatment methods is by managing them in a practical, medicinal environment.

Bibliography

- [1] Paul F Cook and William Wallace Cleland. *Enzyme Kinetics and Mechanism*. Garland Science, 2007.
- [2] Michael C Reed, Anna Lieb, and H Frederik Nijhout. The Biological Significance of Substrate Inhibition: A Mechanism with Diverse Functions. *Bioessays*, 32(5): 422–429, 2010.
- [3] T Drengstig, K Thorsen, IW Jolma, and P Ruoff. Fysiologiske reguleringsmekanismer. *Naturen*, 137(04):128–137, 2013.
- [4] Lisa A Urry, Michael Lee Cain, Steven Alexander Wasserman, Peter V Minorsky, and Jane B Reece. *Biology: A Global Approach (11th Edition)*. Pearson Education, Incorporated, 2017.
- [5] Steven J Cooper. From Claude Bernard to Walter Cannon. Emergence of the concept of homeostasis. *Appetite*, 51(3):419–427, 2008.
- [6] T. Schab. Cannon’s Four features of Homeostasis, 2017. URL <https://classroom.synonym.com/cannons-four-features-homeostasis-41547.html>.
- [7] K Schillo. *Human Anatomy and Physiology: Form, Function, and Homeostasis*. Cognella Academic Publishing, 2018.
- [8] Gérard Eberl. Robustness in Living Organisms is Homeostasis. In *Seminars in Immunology*, volume 36, pages 56–57. 2018.
- [9] T Drengstig, XY Ni, K Thorsen, IW Jolma, and P Ruoff. Robust adaptation and Homeostasis by Autocatalysis. *The Journal of Physical Chemistry B*, 116(18): 5355–5363, 2012.
- [10] Daniela Vallone, Roberto Picetti, and Emiliana Borrelli. Structure and Function of Dopamine Receptors. *Neuroscience & Biobehavioral Reviews*, 24(1):125–132, 2000.
- [11] Michael S Wolfe. Parkinsons Disease and Other α -Synucleinopathies. pages 117–143, 2018.

-
- [12] Krishnan Radhakrishnan and Alan C Hindmarsh. Description and use of LSODE, the Livermore Solver for Ordinary Differential Equations. 1993.
- [13] Montserrat Royo, S Colette Daubner, and Paul F Fitzpatrick. Effects of Mutations in Tyrosine Hydroxylase Associated With Progressive Dystonia on the Activity and Stability of the Protein. *Proteins: Structure, Function, and Bioinformatics*, 58(1): 14–21, 2005.
- [14] Norio Kaneda, Kazuto Kobayashi, Hiroshi Ichinose, Fumio Kishi, Atsushi Nakazawa, Yoshikazu Kurosawa, Keisuke Fujita, and Toshiharu Nagatsu. Isolation of a Novel cDNA Clone for human Tyrosine Hydroxylase: Alternative RNA Splicing Produces Four Kinds of mRNA from a Single Gene. *Biochemical and Biophysical Research Communications*, 146(3):971–975, 1987.
- [15] Shamima Nasrin, Hiroshi Ichinose, Hiroyoshi Hidaka, and Toshiharu Nagatsu. Recombinant Human Tyrosine Hydroxylase Types 1–4 Show Regulatory Kinetic Properties for the Natural (6 R)-Tetrahydrobiopterin Cofactor. *The Journal of Biochemistry*, 116(2):393–398, 1994.
- [16] Giri R Sura, S Colette Daubner, and Paul F Fitzpatrick. Effects of Phosphorylation by Protein Kinase A on Binding of Catecholamines to the Human Tyrosine Hydroxylase Isoforms. *Journal of Neurochemistry*, 90(4):970–978, 2004.
- [17] Mariarita Bertoldi and Carla Borri Voltattorni. Multiple Roles of the Active Site Lysine of Dopa Decarboxylase. *Archives of Biochemistry and Biophysics*, 488(2): 130–139, 2009.
- [18] Mariarita Bertoldi. Mammalian Dopa decarboxylase: Structure, Catalytic Activity and Inhibition. *Archives of Biochemistry and Biophysics*, 546:1–7, 2014.
- [19] Trent J Volz, Glen R Hanson, and Annette E Fleckenstein. Measurement of Kinetically Resolved Vesicular Dopamine Uptake and Efflux using Rotating Disk Electrode Voltammetry. *Journal of Neuroscience methods*, 155(1):109–115, 2006.
- [20] Stefano Fogal, Marcello Carotti, Laura Giaretta, Federico Lanciai, Leonardo Nogara, Luigi Bubacco, and Elisabetta Bergantino. Human Tyrosinase Produced in Insect Cells: A Landmark for the Screening of New Drugs Addressing its Activity. *Molecular Biotechnology*, 57(1):45–57, 2015.
- [21] Montserrat Royo, S Colette Daubner, and Paul F Fitzpatrick. Effects of Mutations in Tyrosine Hydroxylase Associated with Progressive Dystonia on the Activity and Stability of the Protein. *Proteins: Structure, Function, and Bioinformatics*, 58(1): 14–21, 2005.

-
- [22] Hong-Yan Han, Jae-Rin Lee, Wei-An Xu, Myong-Joon Hahn, Jun-Mo Yang, and Yong-Doo Park. Effect of Cl⁻ on Tyrosinase: Complex Inhibition Kinetics and Biochemical Implication. *Journal of Biomolecular Structure and Dynamics*, 25(2): 165–171, 2007.
- [23] Shu Hashimoto, Naojiro Minami, Masayasu Yamada, and Hiroshi Imai. Excessive Concentration of Glucose during in Vitro Maturation Impairs the Developmental Competence of Bovine Oocytes after In Vitro Fertilization: Relevance to Intracellular Reactive Oxygen Species and Glutathione Contents. *Molecular Reproduction and Development: Incorporating Gamete Research*, 56(4):520–526, 2000.
- [24] Jan Haavik. L-DOPA is a Substrate for Tyrosine Hydroxylase. *Journal of Neurochemistry*, 69(4):1720–1728, 1997.
- [25] Joseph Grimsby, Kevin Chen, Li-Jia Wang, Nancy C Lan, and Jean C Shih. Human Monoamine Oxidase A and B Genes Exhibit Identical Exon-Intron Organization. *Proceedings of the National Academy of Sciences*, 88(9):3637–3641, 1991.
- [26] Thomas Jubault, Laura Monetta, Antonio P Strafella, Anne-Louise Lafontaine, and Oury Monchi. L-DOPA Medication in Parkinson’s Disease Restores Activity in the Motor Cortico-Striatal Loop but does not Modify the Cognitive Network. *PLoS One*, 4(7):e6154, 2009.
- [27] Hyone-Myong Eun. *Enzymology Primer for Recombinant DNA Technology*. Elsevier, 1996.
- [28] Anne S Berry, Vyoma D Shah, Suzanne L Baker, Jacob W Vogel, James P O’Neil, Mustafa Janabi, Henry D Schwimmer, Shawn M Marks, and William J Jagust. Aging affects Dopaminergic Neural Mechanisms of Cognitive Flexibility. *Journal of Neuroscience*, 36(50):12559–12569, 2016.
- [29] S. Falck and B. Cadman. Dopamine Deficiency: Symptoms, Causes, and Treatment, 2018. URL <https://www.medicalnewstoday.com/articles/320637>.
- [30] Allison W Willis. Parkinson Disease in the Elderly Adult. *Missouri Medicine*, 110(5):406, 2013.
- [31] Vera Dias, Eunsung Junn, and M Maral Mouradian. The Role of Oxidative Stress in Parkinson’s Disease. *Journal of Parkinson’s Disease*, 3(4):461–491, 2013.
- [32] Michael Schieber and Navdeep S Chandel. ROS Function in Redox Signaling and Oxidative Stress. *Current Biology*, 24(10):453–462, 2014.

-
- [33] Branden J Stansley and Bryan K Yamamoto. L-DOPA-Induced Dopamine Synthesis and Oxidative Stress in Serotonergic Cells. *Neuropharmacology*, 67:243–251, 2013.
- [34] Justin R Nickell, Kiran B Siripurapu, Ashish Vartak, Peter A Crooks, and Linda P Dwoskin. The Vesicular Monoamine transporter-2: an Important Pharmacological Target for the Discovery of Novel Therapeutics to treat Methamphetamine Abuse. *Advances in Pharmacology*, 69:71–106, 2014.
- [35] Thomas S Guillot and Gary W Miller. Protective Actions of the Vesicular Monoamine Transporter 2 (VMAT2) in Monoaminergic Neurons. *Molecular Neurobiology*, 39(2):149–170, 2009.
- [36] Shams Tabrez, Nasimudeen R Jabir, Shazi Shakil, Nigel H Greig, Qamre Alam, Adel M Abuzenadah, Ghazi A Damanhour, and Mohammad A Kamal. A Synopsis on the Role of Tyrosine Hydroxylase in Parkinson’s Disease. *CNS Neurological Disorders-Drug Targets*, 11(4):395–409, 2012.
- [37] Zhen Qi, Gary W Miller, and Eberhard O Voit. Computational Systems Analysis of Dopamine Metabolism. *PLoS One*, 3(6):e2444, 2008.
- [38] S Colette Daubner, Tiffany Le, and Shanzhi Wang. Tyrosine Hydroxylase and Regulation of Dopamine Synthesis. *Archives of Biochemistry and Biophysics*, 508(1):1–12, 2011.
- [39] Sarah L Gordon, Noelene S Quinsey, Peter R Dunkley, and Phillip W Dickson. Tyrosine Hydroxylase Activity is Regulated by two Distinct Dopamine-binding Sites. *Journal of Neurochemistry*, 106(4):1614–1623, 2008.
- [40] Yimei Xu, Alan H Stokes, Robert Roskoski Jr, and Kent E Vrana. Dopamine, in the Presence of Tyrosinase, Covalently Modifies and Inactivates Tyrosine Hydroxylase. *Journal of Neuroscience Research*, 54(5):691–697, 1998.
- [41] Lisette Blanco-Lezcano, Esteban Alberti-Amador, Mei-Li Díaz-Hung, María Elena González-Fraguela, Bárbara Estupiñán-Díaz, Teresa Serrano-Sánchez, Liliana Francis-Turner, Javier Jiménez-Martín, Yamilé Vega-Hurtado, and Isabel Fernández-Jiménez. Tyrosine Hydroxylase, Vesicular Monoamine Transporter and Dopamine Transporter mRNA Expression in Nigrostriatal Tissue of rats with P-dunculopontine Neurotoxic Lesion. *Behavioral Sciences*, 8(2):20, 2018.
- [42] K Kompolti and Leo V Metman. *Encyclopedia of Movement Disorders*. Elsevier, 2010.

- [43] Phillip Mackie, Joe Lebowitz, Leila Saadatpour, Emily Nickoloff, Peter Gaskill, and Habibeh Khoshbouei. The dopamine transporter: An Unrecognized Nexus for Dysfunctional Peripheral Immunity and Signaling in Parkinson's Disease. *Brain, Behavior, and Immunity*, 70:21–35, 2018.
- [44] Christopher P Ford. The Role of D2-autoreceptors in Regulating Dopamine Neuron Activity and Transmission. *Neuroscience*, 282:13–22, 2014.
- [45] Shin Hisahara and Shun Shimohama. Dopamine Receptors and Parkinson's Disease. *International Journal of Medicinal Chemistry*, 2011, 2011.
- [46] Nicholas Mrosovsky. *Rheostasis: The Physiology of Change*. Oxford University Press, 1990.